

Carbon

March 2018, Volume 128 Pages 54-62

<https://doi.org/10.1016/j.carbon.2017.11.060><https://archimer.ifremer.fr/doc/00476/58747/>**Archimer**<https://archimer.ifremer.fr>

Transformation of C-60 fullerene aggregates suspended and weathered under realistic environmental conditions

Sanchis Josep ¹, Aminot Yann ², Abad Esteban ¹, Jha Awadhesh N. ², Readman James W. ^{2,3}, Farre Marinella ^{1,*}

¹ CSIC, IDAEA, Inst Environm Assessment & Water Res, Water & Soil Qual Res Grp, C Jordi Girona 18-26, Barcelona 08034, Catalonia, Spain.

² Plymouth Univ, Biogeochem Res Ctr, Plymouth PL4 8AA, Devon, England.

³ Plymouth Marine Lab, Prospect Pl, Plymouth PL1 3DH, Devon, England.

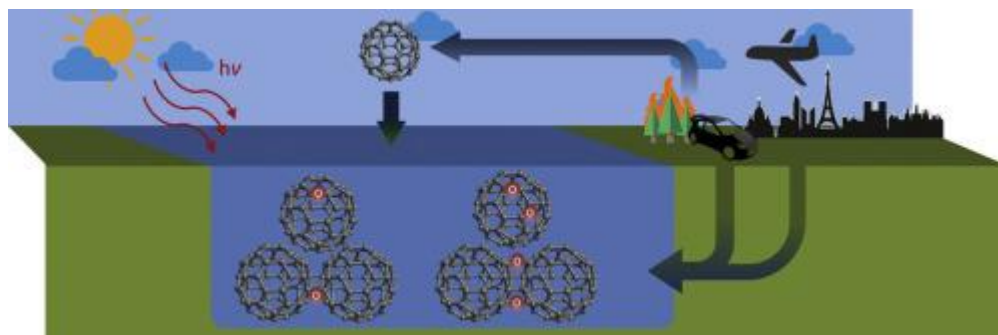
* Corresponding author : Marinella Farre, email address : mfugam@cid.csic.es

Abstract :

The occurrence, fate and behaviour of carbon nanomaterials in the aquatic environment are dominated by their functionalization, association with organic material and aggregation behaviour. In particular, the degradation of fullerene aggregates in the aquatic environment is a primary influence on their mobility, sorption potential and toxicity. However, the degradation and kinetics of water suspensions of fullerenes remain poorly understood.

In the present work, first, an analytical method based on liquid chromatography and high-resolution mass spectrometry (LC-HRMS) for the determination of C-60 fullerene and their environmental transformation products was developed. Secondly, a series of C-60 fullerene water suspensions were degraded under relevant environmental conditions, controlling the salinity, the humic substances content, the pH and the sunlight irradiation. Up to ten transformation products were tentatively identified, including epoxides and dimers with two C-60 units linked via one or two adjacent furane-like rings. Fullerenols were not observed under these environmentally relevant conditions.

The kinetics of generation of each transformation product were studied with and without simulated sunlight conditions. The ionic strength of the media, its pH and the humic substances content were observed to modulate the kinetics of generation.

Graphical abstract

37

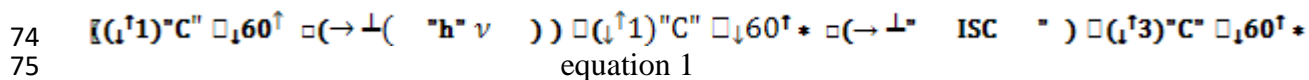
38 1. Introduction

39 Since its discovery [1], C₆₀ fullerene stands as one of the most deeply studied carbon-
40 based nanomaterial. Nowadays, C₆₀ fullerene and its derivatives have been proposed for
41 use in medical applications [2, 3], in analytical chemistry [4, 5], in microelectronics
42 components [6, 7], in solar cells' bulk hetero-junctions[8, 9] and as a component of a
43 wide diversity of nanocomposites [10, 11]. In addition, fullerenes, together with other
44 carbon nanomaterials, may be generated in highly energetic events of either natural or
45 anthropogenic nature, including lightning discharges [12], meteorite (chondrite) impacts
46 [13, 14], forest fires [15, 16], candles [17] and car engines [18]. The last consequence of
47 all of these processes is the emission of fullerenes into the environment [19-26], where
48 they are distributed amongst its different compartments.

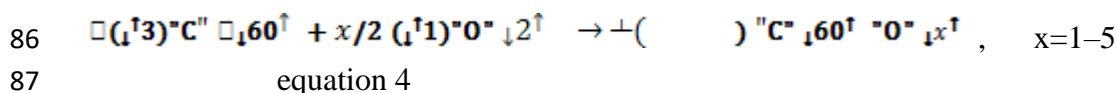
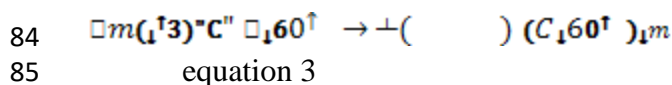
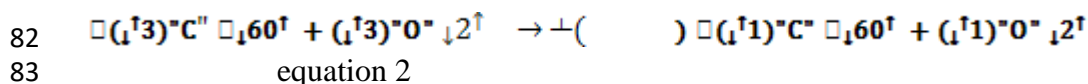
49 The analysis of fullerenes in the environment is a relatively recent topic. From an
50 analytical perspective, their analysis is challenging because of their extremely low
51 environmental levels [27], the need for specific instrumentation, and their
52 hydrophobicity. Besides, mass spectrometric analysis of fullerenes has some unique
53 challenges: low ionization efficiencies are obtained with both electrospray ionisation
54 (ESI) and atmospheric pressure chemical ionisation (APCI) sources and, in addition, the
55 fragmentation of fullerenes by tandem mass spectrometers is virtually non-existent.
56 Therefore, methods based on atmospheric pressure photoionization (APPI) sources and
57 high resolution mass spectrometry (HRMS) are preferred [19, 21, 28]. Recent analytical
58 approaches have allowed lower detection limits [29], and the occurrence of C₆₀S has
59 been reported in rivers and ponds at low ng l⁻¹ and sub-ng l⁻¹ concentrations [21-24, 28].
60 Despite the extreme hydrophobicity of this molecule (log K_{OW}=6.67 [30]), C₆₀ fullerene
61 can be stabilized in water because (1) C₆₀ is a strong sorbent material that is readily
62 attached to suspended matter [31] and (2) fullerene molecules aggregate creating
63 clusters [32] (termed herein as nC₆₀), the surfaces of which are surrounded by a “*stable*
64 *spherical shell of interconnected water molecules*” [33].

65 It is well known that the colloidal behaviour of nC₆₀ responds to the Derjaguin-Landau-
66 Verwey-Overbeek (DLVO) model [34-36]. The stabilization of nC₆₀ is attributed to
67 repulsive van der Waals forces, but it is unclear to what extent the chemical
68 functionalization of the aggregates' surface plays a role in the stability of nC₆₀ in the

69 real environment. For instance, it is known that UV irradiation induces chemical
 70 changes in nC₆₀ surfaces and enhances the stability of nC₆₀ in water [37, 38]. This can
 71 be attributed to the excitation of C₆₀ fullerene to singlet C₆₀ (¹C₆₀), which in turn is
 72 converted into triplet C₆₀ (³C₆₀) via intersystem crossing (ISC), as described in equation
 73 1.



76 This mechanism was initially studied in benzene suspension by Arbogast *et al.* (1991)
 77 [39] and was later observed in aqueous suspension [40, 41]. Once generated, triple
 78 excited C₆₀ undergoes several reactions, including self-quenching with ambient oxygen,
 79 which generates singlet oxygen and singlet C₆₀ (equation 2); C₆₀ oligomerization, via
 80 [2+2] cycloaddition (equation 3); and C₆₀ functionalization, such as the formation of a
 81 variety of epoxides (equation 4) [42, 43].



88 The production of these transformation products is dependent on two main factors: the
 89 type of irradiation and to the presence of ozone. With regards to the former, under
 90 strong irradiation conditions, reactions occur relatively quickly, whilst under natural
 91 sunlight they happen during weeks/months [44]. In addition, under harsh irradiation
 92 conditions, other transformation products have been observed, such as the C₆₀
 93 dicarbonyl [45], and even the breakdown of the fullerene carbon cage [46]. With
 94 regards to the presence of ozone, Fortner *et al* (2007) observed the high reactivity of
 95 nC₆₀, which resulted in the formation of oxidised transformation products with up to 29
 96 oxygen atoms. Heymann *et al.* described the generation of the relatively stable [6,6]-
 97 closed C₆₀ epoxide, upon ozonolysis, via decomposition of the intermediate [6,6]-closed
 98 C₆₀ ozonide (C₆₀O₃) [47]. Murdianti *et al.* (2012) detected significant concentrations of
 99 the same [6,6]-closed C₆₀ epoxide after the exposure to common ozone concentrations,
 100 under ambient air exposure [48].

101 The wide variety of (photo)transformation products and the influence of ambient factors
102 on their generation underpin the need to faithfully reproduce realistic environmental
103 conditions in order to unambiguously identify which C₆₀ fullerene transformation
104 products are generated in the real environment, to study their kinetics and, ultimately, to
105 study their occurrence in real samples. This topic has recently been addressed in air [49]
106 and soil [50] matrices, but has not been systematically assessed in waters with different
107 physicochemical properties.

108 In the present study, an analytical method based on high performance liquid
109 chromatography coupled to high resolution mass spectrometry (HPLC-HRMS) was
110 developed for the analysis of C₆₀ transformation products. C₆₀ was dispersed by long
111 term stirring in artificial water media (containing environmentally relevant pH values,
112 salt compositions and humic acid contents) and nC₆₀ were exposed, under atmospheric
113 condition, to controlled sunlight or dark conditions. The presence of environmentally
114 relevant transformation products and their kinetics of formation were assessed.

115

116 **2. Experimental section**

117 **2.1. Reagents and chemicals** A standard of C₆₀ fullerene (sublimed, 99.9 % purity; ref.
118 572500) was purchased from Sigma-Aldrich (Steinheim, Germany). ¹³C-enriched C₆₀
119 fullerene (>99 % purity; ref. MRL613), containing 45–55 % of ¹³C atoms in each C₆₀
120 molecule (¹³C₂₇¹²C₃₃–¹³C₃₃¹²C₂₇) was purchased from MER Corporation (Tucson, AZ,
121 USA). The molecule ¹³C₃₀¹²C₃₀ (m/z of its molecular radical anion, 750.1012) was used
122 as an internal standard. Standards of humic acids (technical grade, reference 53680) and
123 salts (including CaCl₂, CaCl₂·2H₂O, H₃BO₃, KBr, KCl, MgCl₂, MgCl₂·6H₂O, NaCl,
124 NaF, NaHCO₃, Na₂SO₄, and SrCl₂·6H₂O) were purchased from Sigma-Aldrich
125 (Steinheim, Germany).

126 With respect to the solvents used in the extraction: methanol (LiChrosolv®) was
127 supplied by Merck (Darmstadt, Germany); dichloromethane, toluene and ethyl acetate
128 (“for organic residue analysis” grade) were purchased from J.T.Baker (Deventer, The
129 Netherlands); and 1,2-dichlorobenzene (anhydrous, 99 %) and 1-butyl-3-
130 methylimidazolium hexafluorophosphate ([BMIM][PF₆], ≥97.0 %) were purchased
131 from Sigma-Aldrich (Steinheim, Germany). Concerning solvents for chromatography:
132 methanol, ultrapure water (UPW) and acetonitrile (Optima® LC/MS grade) were
133 purchased from Fischer Chemical (Loughborough, UK), while toluene (Chromasolv®)
134 and *n*-hexane (SupraSolv®) were purchased from Merck (Darmstadt, Germany).

135 **2.2. Preparation of the fullerene suspensions** 1.0 ± 0.05 mg of C₆₀ fullerene powder
136 was weighed in tared quartz vials. 20.0 ± 0.02 ml of the corresponding water medium
137 were pipetted inside each vial, obtaining a suspension with a concentration 50 ± 2.5 mg
138 l⁻¹ (~69 ± 3.5 μM). Vials were loosely capped with previously slitted aluminium foil,
139 allowing free ambient air exchange while preventing potential contamination from dust
140 deposition.

141 Nine different media were prepared, simulating different environmental scenarios (see
142 **Table 1**). Suspensions 1, 2 and 3 allowed the study of the effects of salinity;
143 suspensions 1, 4 and 5 allowed the study of the effects of pH; and suspensions 1, 6 and
144 7 allowed the study of the effects of humic substances content. These three parameters
145 are known to control the colloidal chemistry of nC₆₀ [32, 51, 52] and, subsequently, the

146 number of C₆₀ molecules located in the surface of the aggregates. In addition,
147 experiment 8, reproducing artificial freshwater (AFW), and experiment 9, artificial
148 seawater (ASW), were also conducted. The salinity, the pH and the concentration of
149 humic acids were studied because they have been shown to regulate the size of nC₆₀
150 aggregates [32, 51, 52], which can be a relevant factor if we assume that
151 functionalization of fullerenes is a surface reaction.

152 Media with a high ionic strength (46,000 μS cm⁻¹, suspensions 3 and 9) were prepared
153 in order to simulate the salinity of seawater [53] by dissolving NaCl (23.93 g l⁻¹),
154 MgCl₂·6H₂O (10.80 g l⁻¹), Na₂SO₄ (4.01 g l⁻¹), CaCl₂·2H₂O (1.50 g l⁻¹), KCl (0.677 g l⁻¹),
155 NaHCO₃ (196.0 mg l⁻¹), KBr (98.0 mg l⁻¹), H₃BO₃ (26.0 mg l⁻¹), SrCl₂·6H₂O (24.0
156 mg l⁻¹), and NaF (3.0 mg l⁻¹) in UPW. Media with an intermediate ionic strength (970
157 μS/cm, suspensions 2 and 8) were prepared according to Lipschitz and Michel (2002)
158 [54] by dissolving NaCl (175.3 mg l⁻¹), CaCl₂ (22.2 mg l⁻¹), MgCl₂ (19.0 mg l⁻¹) and
159 KCl (14.9 mg l⁻¹) in UPW. The remaining suspensions were prepared with UPW (5.8
160 μS/cm), adjusting the humic acid contents and the pH with NaOH(aq) and HCl(aq)
161 when necessary.

162 **2.3. Weathering, sampling and extraction** Two series of experiments were performed:
163 one with sunlight irradiation and another in dark conditions. Quartz vials for irradiated
164 experiments were gently vortexed during 1.0 min and placed in a SunTest apparatus
165 from Heraeus (Hanau, Germany), equipped with a Xenon arc lamp that provided an
166 irradiance of 600 W m⁻² ($E_{e\lambda=365\text{ nm}} = 3.180\text{ mW cm}^{-2}$ and $E_{e\lambda=312\text{ nm}} = 2.283\text{ mW cm}^{-2}$).
167 Quartz vials for non-irradiated experiments were covered with aluminium foil, placed in
168 a 10-position magnetic stirrer and agitated with PTFE-coated magnetic bars.

169 Aliquots were taken from each vial periodically until the experiments were finalized,
170 after 48 and 96 hours for the irradiated and the non-irradiated series, respectively. The
171 optimization of the extraction method is described in the Supplementary Information
172 (Text S1). Briefly, 500 μL of sample were placed in a 3 ml glass vial containing 1.00
173 ml of toluene spiked with ¹³C-enriched C₆₀ fullerene at a concentration of 10 ng mL⁻¹.
174 The vial was capped and vortexed during 1 min. After separation of phases, an aliquot
175 of ~1 ml of toluene extract was transferred with a Pasteur pipette into a 1.5 ml amber
176 LC vial for its instrumental analysis

177 **2.4. Instrumental analysis** The HPLC-HRMS method was based on a previously
178 published one [21]. Some modifications were introduced in order to optimize the
179 separation and detection of C₆₀ transformation products.

180 The optimization of the HPLC-HRMS method is described in the Supplementary
181 Information (**Texts S2 and S3**). HPLC separation was achieved by non-aqueous LC,
182 using an Acquity UPLC System (Waters, Milford, MA, USA) equipped with a
183 COSMOSIL™ Buckyprep column (150 × 2.0 mm; particle size, 5 μm; pore size, ~120
184 Å) from Nacalai Tesque Inc. (Kyoto, Japan). The mobile phase consisted of an isocratic
185 flow of toluene and methanol, at a 9 to 1 ratio, flowing at 0.4 ml.min⁻¹ during 20 min.
186 20 μl of extract was injected in each run.

187 The system was coupled to a Q Exactive™ mass spectrometer (Thermo Fischer
188 Scientific, San Jose, CA, USA) with a hybrid atmospheric pressure chemical ionisation /
189 atmospheric pressure photoionisation (APCI/APPI) source Ion Max (Thermo Fischer
190 Scientific, San Jose, CA, USA) working in APPI mode. Ionisation was carried out in
191 negative polarity and source parameters were set as follows: sheath gas, 40 a.u.;
192 auxiliary gas, 25 a.u.; spare gas, 1 a.u.; spray voltage, 5.0 kV; capillary and probe heater
193 temperatures, 300 °C and 400 °C, respectively; and S-lens RF, 90 %. Acquisition was
194 performed in full scan from m/z = 300 to 1,600 with a resolution of 140,000 full width
195 at half maximum (FWHM).

196 **2.5. Precautions and safety considerations** Precautions and safety considerations are
197 summarised in the **Text S4** of the Supplementary Information.

198

199 **3. Results and discussion**

200 **3.1. Identification of transformation products** Up to ten transformation products of
201 C₆₀ fullerene were detected (see **Table 2**). All the experimental m/z signals could be
202 tentatively assigned to empirical formulae with mass accuracies <1.5 ppm (<0.5 ppm, in
203 those molecules smaller than 1,000 Da). The identified compounds also presented the
204 isotopic patterns of C₆₀ (with a predominant [¹²C₆₀]⁻ signal, followed by the signals
205 [¹²C₅₉¹³C]⁻ and [¹²C₅₈¹³C₂]⁻, with relative intensities of ~0.65 and ~0.22, respectively)
206 or C₁₂₀ (with a predominant [¹²C₁₁₉¹³C]⁻ signal, and the signals [¹²C₁₂₀]⁻ and [¹²C₁₁₈
207 ¹³C₂]⁻ with relative intensities of ~0.77 and ~0.64).

208 The tentatively identified compounds included several oxidized fullerenes, one mono-
209 oxidized dimer of C₆₀ fullerene and three signals corresponding to dioxidized dimers of
210 C₆₀ fullerenes. Standards of these compounds were not commercially available.

211 A single peak of mono-oxidised fullerene was observed with a retention time of 3.50
212 min (see **Figure 1b**). The structural isomers that can be assigned to the formula C₆₀O
213 are the C₆₀ epoxide (abbreviated [6,6]C₆₀O) and the C₆₀ oxido-annulene (abbreviated
214 [5,6]C₆₀O) [55], both represented in the **Figure S5** of the Supporting Information. Both
215 molecules can be generated by oxidation, under harsh oxidative conditions, i.e. with
216 dimethyldioxirane [56], or by reaction with ozone, as reported before [57]. While the
217 thermolysis of the ozonide intermediate produces [6,6]C₆₀O, its photolytic scission
218 produces [5,6]C₆₀O. Therefore, [6,6]C₆₀O is likely to be predominant in dark
219 experiments, while [5,6]C₆₀O would be formed by irradiation but the simultaneous
220 generation of both products cannot be excluded.

221 The other two peaks in **Figure 1.b**, with retention times (t_R) of ~2 and 3.07 min
222 corresponded to a matrix interference and to an APPI-adduct of the C₆₀ peak,
223 respectively.

224 Three C₆₀O₂ signals were observed: one peak at $t_R=3.73$ ($k'=3.0$), another at $t_R=6.92$
225 ($k'=6.2$) and a third signal at $t_R=8.71$. While the third peak is believed to be a
226 chromatographic artefact (attributed to the in-source fragmentation of C₆₀O₃) the first
227 two peaks can be assigned to transformation products, either C₆₀ dicarbonyl and to
228 diepoxidized C₆₀. The C₆₀ dicarbonyl is generated by decomposition of the C₆₀
229 dioxetane, a highly unstable intermediate produced by the addition of a ¹O₂ to a C₆₀'s
230 [6,6] bond [45]. Nevertheless, the C₆₀ dicarbonyl is unlikely to be generated in the
231 present experiments since its precursor, the C₆₀ dioxetane, is only generated under harsh
232 irradiation conditions. The presence of epoxy groups instead of carbonyl groups on
233 mono-, di- and tri-oxidised fullerenes was also confirmed by FTIR and ¹³C NMR after
234 light exposure in solution [58]. More likely, the two peaks belong to any of the eight
235 regioisomers of diepoxidized C₆₀ fullerene that can exist [59] (see **Figure 2**). In
236 previous works two chromatographic peaks have been also reported corresponding to
237 diepoxides of C₆₀ fullerene, after reaction with *m*-chloroperoxybenzoic acid [59, 60] or
238 with ozone [61]. While the predominant peak has been previously identified as the
239 isomer *cis1*, which is also the most stable diepoxide according to computational

240 calculations [60, 62], the less intense peak has been assigned to an unresolved mixture
241 of diepoxidized fullerenes [59], to the equatorial isomer [60], and to the isomer *cis2*
242 [61]. Therefore, the peak at $k'=3.0$, which was the predominant one in all the
243 experiments, was assigned to the *cis1* regioisomer, while the peak at $k'=6.2$ may be
244 either the *cis2* or the *equatorial* isomer. To further characterize both diepoxides, the
245 toluene extract was fractionated and the fractions corresponding to the first and second
246 peaks were analysed by infrared (IR) spectroscopy. However, due to the low
247 concentrations and to the interference from column bleed, non-conclusive results were
248 obtained.

249 As can be seen in **Figure 1d**, four signals were detected with the m/z of trioxidized C_{60}
250 fullerenes. The signals at $t_R=3.73$ and $t_R=6.92$ min are APPI-adducts of $C_{60}O_2$ isomers,
251 which have already been described. In contrast, the other two signals belong to new
252 transformation products ($k'=3.8$ and $k'=6.4$, the second one being the most intense). The
253 presence of the ozonide $C_{60}O_3$ was discarded because of its instability [63]. Instead,
254 according to previous theoretical and experimental works [60, 62, 64], the presence of
255 different isomers of the triepoxidized C_{60} fullerene was considered. Among the 43
256 possible regioisomers of triepoxidized C_{60} fullerene, the most abundant was the one that
257 contains the three oxygen atoms in the [6,6] bonds of the same benzene ring (C_{3v}
258 symmetry, see **Figure S6a**), which is thermodynamically favoured [65]. The least
259 abundant detected compounds were likely to present the three epoxide groups in
260 adjacent [6,6] bonds (see **Figures S6b** and **S6c**): two groups in the same benzene ring
261 and the third group in the most nearby [6,6] bond of an adjacent benzene ring.

262 Similarly, a single tetraoxidized transformation product was detected (see **Figure S7**).
263 To our knowledge, the stability and relative predominance of the C_{60} tetraepoxide
264 regioisomers has not been addressed to date in any previous work. According to the
265 stability criteria that have been employed for the triepoxides discussion, the most stable
266 regioisomer of the tetraepoxides family should be the one with three functional groups
267 in the same benzene ring and the fourth epoxide group in an adjacent [6,6] bond.
268 Epoxides with formula $C_{60}O_5$ or $C_{60}O_6$ have been observed elsewhere after 1-3 minutes
269 of ozonolysis [66], but were short-lived. IR evidence of cage rupture was found for high
270 degree of oxygenation [67]. The softer oxidation conditions employed in our work
271 could also account for their nondetection.

272 The formation of four fullerene dimers was also observed (**Figure 3**), corresponding to
273 a compound with formula $(C_{60})_2O$ and three compounds with formula $(C_{60})_2O_2$. The
274 signal of $(C_{60})_2O$ ($k'=7.2$) was already elucidated [68] (see chromatogram and proposed
275 structure in **Figure 4**). This compound is generated by [2+2] reaction of [6,6] $C_{60}O$ with
276 the [6,6] bond of a C_{60} fullerene, originating a molecule with two C_{60} units linked by a
277 furane-like ring.

278 Regarding $(C_{60})_2O_2$, three different chromatographic peaks were observed (I, II and III
279 in **Figure 3**). The peak I ($k'=8.2$) appeared as a well-resolved chromatographic peak
280 while the peaks II ($k'=15.5$) and III ($k'=19.2$) corresponded to mixtures of
281 chromatographically unresolved isomers. Two different types of structures could be
282 assigned to these three peaks: an epoxidized $(C_{60})_2O$, which may be produced either by
283 the [2+2] reaction of two [6,6] $C_{60}O$ molecules or by epoxidation of a $(C_{60})_2O$ molecule;
284 or a bis-linked compound, consisting in two C_{60} units fused via two adjacent furane-like
285 rings. The furane-like rings links may be separated by [6,6] bonds or by [5,6] bonds, as
286 described elsewhere [69]. In this case, the assignment of a structure to each peak was
287 less clear. On the basis of the retention of each peak and the polarity of the compounds,
288 peak I may be the bis-linked compound, while peaks II and III were most likely related
289 to a mixture of regioisomers, as described in **Figure 3**.

290 In a previous work, $(C_{60})_2O$ and $(C_{60})_2O_2$ have been identified as degradation products
291 of C_{60} fullerene in solid state [70]. Also, the presence of dimerized fullerenes were
292 suspected after UV-spectroscopy analyses in aerosol samples degraded with ozone [69].
293 However, according to our knowledge, this is the first time that fullerene dimers are
294 unambiguously proven to be a component of nC_{60} produced under environmentally
295 relevant conditions. Neither $(C_{60})_2$ nor any molecule containing more than two sub-units
296 of C_{60} fullerene were detected in the present work.

297 Finally, hydroxylated fullerenes, or fullerenols, were not detected in any degradation
298 experiment, including the analysis of the toluene extracts, the analysis of extracts by
299 other organic solvents (see **Text S1**) and the analysis of water suspensions by direct
300 injection inside the mass spectrometer. The use of an electrospray source, which has
301 been used elsewhere for analysing these compounds [71], was also fruitless. In the
302 literature, fullerenols were recently reported in soils incubated under ultraviolet
303 irradiation [50] and in water suspensions prepared by direct sonication without light

304 exposure [72, 73]. Therefore, in a complementary experiment, a C₆₀ suspension was
305 prepared in ultrapure water at pH 12 and was sonicated in an ultrasonic bath for 1 hour.
306 After extraction with toluene, the analysis of the extract revealed a series of prominent
307 peaks with molecular ions [C₆₀O_xH_(x-1)]⁻ (x=1-6), presumably belonging to
308 deprotonated fullerenols. The intensities of these signals were ~10⁴ times lower than
309 that of the precursor, C₆₀ fullerene, and, as can be seen in **Figure S8**, all the fullerenols
310 eluted at a lower retention time than C₆₀ (selectivity $\alpha \leq 0.55$), in contrast to the other
311 compounds listed in **Table 2**. It can be concluded that fullerenols are not produced in
312 water suspension in normal environmental conditions, as it was not observed previously
313 in ultrapure water [48].

314 **3.2. Kinetics of degradation of C₆₀ fullerene in ultrapure water** **Table 3** summarizes
315 the results obtained when plotting the concentration of fullerene epoxides against the
316 time of experiment. The concentrations of the degradation products were normalized by
317 the concentration of precursor C₆₀, as justified in the **Supplementary Text S5** and
318 **Figure S9**

319 The presence or absence of sunlight affected decisively the generation of epoxides.
320 Higher concentrations of transformation products were observed in experiments with
321 sunlight in comparison to experiments in the dark. E.g., concentrations of C₆₀O₄, C₆₀O₃
322 ($k'=3.8$) and C₆₀O₃ ($k'=6.4$) were 19±11, 7.3±5.5 and 2.9±1.3 times higher in the
323 presence of sunlight than in the dark.

324 In irradiated experiments, during the initial hours, the concentration of epoxides
325 increased rapidly and more or less linearly; then, it reached a maximum concentration,
326 which in experiments performed in ultrapure water was observed at ~1.5 h); and, during
327 the following 46.5 hours the concentration of epoxides stabilized or decreased (see
328 **Figures S10** and **S11**).

329 In contrast, in experiments without simulated sunlight irradiation, the concentration of
330 epoxides increased steadily and linearly during the 96 hours of the experiment. This
331 general behaviour was observed for all the detected epoxides except for C₆₀O₃ ($k'=3.8$),
332 which reached a peak concentration after only 24 hours of agitation and stabilized.

333 As can be seen in **Table 3**, the generation of epoxides was much slower in the dark (the
334 slopes of the linear regressions are two orders of magnitude lower than in the irradiated

335 experiment). Therefore, the epoxidation of fullerenes was catalysed by light, but light
336 exposure itself was responsible for the disappearance of these compounds after 72
337 hours. This suggests that the stability of fullerene epoxides is limited, but the identity of
338 the next generation of transformation products remains unknown. The generation of
339 higher epoxides, or even open-cage transformation products, can be hypothesized.

340 With regards to dimers with one and two furane-like rings, their generation in ultrapure
341 water experiments, with and without sunlight irradiation, can be seen in **Figure S10**. As
342 can be seen (**Figure S10.a**), $C_{120}O$ was not found in experiments without light
343 irradiation. Its generation may be too slow to be observed under these conditions.
344 When simulated sunlight was applied, $C_{120}O$ was detected after 6 hours and its
345 concentration increased linearly (in ultrapure water, $r=0.95$, $p=0.013$) with an apparent
346 constant of $2.62 \times 10^{-7} \text{ h}^{-1}$. This slope was the flattest of all the compounds, 20 times
347 smaller than that of $C_{60}O_3$ ($k'=3.8$), which was the least abundant epoxide detected.
348 $C_{120}O$ was not only the least abundant degradation product of C_{60} but it also was the
349 only one that increased monotonically through time. This could potentially become a
350 useful tool for dating the presence of C_{60} fullerene in the environment.

351 Finally, $C_{120}O_2$ ($k'=8.2$) was detected in both types of experiments, when suspended in
352 the dark and with light exposure, but a different behaviour was observed in each case.
353 The dimer was generated by solvation and, in the dark, its concentration remained stable
354 during the first 48 hours, after which it increased significantly (see **Figure S10.b**). In
355 contrast, when irradiated, the concentration of $C_{120}O_2$ decreased significantly (see
356 **Figure S10.d**), indicating the lability of this compound.

357 **3.3. Role of salinity, humic acids and pH** As detailed in **Table 1**, degradation
358 experiments were performed at three conductivities (5.8, 970 and 46,000 $\mu\text{S cm}^{-1}$), at
359 three pHs (6.00, 7.00 and 8.15), and with varying concentrations of humic acids (0, 0.3
360 and 2.25 mg l^{-1}). Overall, drastic differences were not observed when modifying these
361 parameters, since the profile of transformation products and their general behaviour
362 remained unchanged, and these physicochemical properties just modulated the results
363 obtained.

364 Regarding salinity, in experiments without light exposure, higher ionic strengths
365 resulted in higher concentrations of epoxides and dimers (**Figure S11**). This trend
366 cannot be satisfactorily explained by the DLVO theory. According to this model, an

367 increase in the salinity of the medium leads to the suppression of the electric double
368 barrier of the aggregates, which favours the dominance of the attractive van der Waals
369 forces among nC₆₀. In this scenario, larger aggregates are stabilized, with smaller
370 surface-to-volume ratio. Assuming that functionalization is a surface reaction, larger
371 aggregates would generate less TPs. However, the opposite was observed in the present
372 work. Our hypothesis is that a higher ionic strength leads to a less negative ζ -potential
373 [74]. In this scenario, the water molecules surrounding the aggregates would be oriented
374 in a more flexible manner, enhancing the diffusion potential of the reactive species as
375 dissolved ozone and ¹O₂.

376 In contrast to all this, irradiated experiments were not affected by changes in the
377 medium salinity.

378 Regarding pH, in experiments without irradiation it was inversely related to the
379 concentration of transformation products. Slightly lower concentrations of
380 transformation products were identified at pH=8.15 than at pH=6.00 (**Figure S12**).
381 Again, irradiated experiments were not significantly affected by changes of the pH.

382 Finally, the presence of humic acids, which are known to modulate the size and shape of
383 nC₆₀ aggregates [38, 75], had an impact on the formation of TPs when irradiated by
384 simulated sunlight: The concentration of epoxides increased with higher concentrations
385 of humic acids and decreased after 24 h of irradiation, while the concentrations of
386 dimers were barely affected (**Figure S13**). This can be attributed to the fact that humic
387 substances, when irradiated with ultraviolet light (especially from UV-A and UV-B
388 regions) can produce reactive oxygen species (ROS) such as ¹O₂, O₂, or H₂O₂ [76].
389 Irradiated humic acids generate radicals that enhance the epoxidation of fullerenes, as
390 observed in the present work. In absence of light, the concentration of humic acids did
391 not present any effect in the generation of TPs.

392 **3.4. Environmental implications** The presence of salts and organic matter in natural
393 waters favours the presence of fullerene transformation products (epoxides and dimers).
394 This was corroborated in the experiments performed in AFW (suspension 8: 970 μ S/cm,
395 pH=7.00 \pm 0.01 and [HA]=2.25 mg l⁻¹) and ASW (suspension 9: 46,000 μ S/cm,
396 pH=8.15 \pm 0.01 and [HA]=0.3 mg l⁻¹), as can be seen in **Figure 4**.

397 The presence of fullerene epoxides and dimers in the real environment is of relevance,
398 given the different properties and behaviour of these transformation products. It is
399 known that functionalised carbon nanotubes and fullerenes adsorb pollutants onto their
400 surfaces with stronger binding than bare nanotubes [77, 78]. Therefore, the potential of
401 fullerenes of immobilizing and transporting other co-contaminants in the aquatic
402 environment is likely to increase progressively after their disposal and weathering [79,
403 80]. This may affect the ecosystem indirectly, by changing the bioavailability of these
404 other co-contaminants, and also directly, because of the different toxicity of fullerenes
405 and fullerene epoxides. In this regard, recent studies have found relevant differences in
406 soil microbial communities when exposed to unaltered nC₆₀ and photodegraded nC₆₀
407 [81]. Also, the presence of functional groups on the surface of the aggregates may
408 enhance their stability in water. This would have implications in the transport potential
409 and water-sediment partition coefficients of fullerenes, as studied elsewhere [21].

410 It is also important to study toxicity, behaviour and sorption capabilities of fullerene
411 dimers to fully understand the implications of their photo-transformation in the real
412 environment.

413 However, in the environment the occurrence of transformation products may be limited,
414 since C₆₀ fullerene seems to be comparatively stable (see the relative abundances of
415 epoxides in **Table 2**). Moreover, sunlight showed an ambivalent effect on the
416 generation of epoxides: whilst it accelerated their generation at first, it also enhanced
417 their elimination after ~24 hours. Therefore the persistence of these transformation
418 products in the environment is likely to be limited. This excludes surface waters located
419 in shady areas, deeper waters, groundwater and closed wells, where the epoxidation of
420 fullerenes would be lower and increase linearly as suggested in our simulations without
421 light exposure.

422 With respect to the persistence of these compounds, it may also be important to consider
423 the role of hetero-aggregation, i.e. their persistence/degradability in presence of
424 inorganic particulate material. Particulate matter/turbidity in a water column may scatter
425 incident light, greatly reducing penetration of light beneath the surface [82]. Therefore,
426 fullerene epoxides may be photodegraded more slowly when they are attached to
427 particles than when they are freely suspended as fullerene homo-aggregates.

428 Moreover, the concentrations of fullerene C₆₀ transformation products may be
429 significantly higher close to the disposal point of wastewater treatment plants, where
430 they may act as pseudo-persistent pollutants. This point was confirmed in a real sample
431 from the Besòs River (close to Barcelona) taken near a wastewater disposal point. 35 l
432 of surface water were spiked with ¹³C₆₀ and extracted by LLE with toluene in a 10:1
433 ratio. The extract was concentrated to 1.0 ml by rotatory evaporation and injected. C₆₀O
434 was detected and determined semi-quantitatively, resulting in an approximate
435 concentration of ~2 ng l⁻¹ (see chromatogram in **Figure S14**). The environmental effects
436 of fullerene transformation products, if confirmed, may be more pronounced on a local-
437 scale in hotspots like this.

438 **Acknowledgements**

439 This work was supported by the Spanish Ministry of Economy and Competitiveness,
440 through the project NANO-transfer (ERA-NET SIINN PCIN-2015-182-CO2-01); by
441 the UK Natural Environment Research Council, through the project “Trojan horses”
442 (NE/L006782/1); and by the Generalitat de Catalunya (Consolidated Research Groups
443 “2014 SGR 418 – Water and Soil Quality Unit” and “2014 SGR 291 – ICRA”). The
444 authors would like to acknowledge the helpful assistance of Dr. Chaler and Mrs. Fanjul
445 from the mass spectrometry services of IDAEA-CSIC.

446 **Conflict of interest**

447 The authors state that there are not actual or potential conflicts of interest.

448

449 **Table 1.** Experimental design showing the salinity, pH and humic acid concentration
 450 (c_{HA}) of the aqueous dispersant media.

#	Description	Conductivity ($\mu\text{S/cm}$)	pH	c_{HA} (mg l^{-1})
Experiment 1	Reference pure water	5.8	7 ± 0.1	0
Experiment 2	Intermediate salinity	970	7.00 ± 0.01	0
Experiment 3	High salinity	46,000	7.00 ± 0.01	0
Experiment 4	Acidic pH	<200	6.00 ± 0.01	0
Experiment 5	Basic pH	<200	8.15 ± 0.01	0
Experiment 6	High c_{HA}	5.8	7 ± 0.1	2.25
Experiment 7	Intermediate c_{HA}	5.8	7 ± 0.1	0.3
Experiment 8	Artificial freshwater	970	7.00 ± 0.01	2.25
Experiment 9	Artificial seawater	46,000	8.15 ± 0.01	0.3

Table 2. Summary of transformation products and their tentatively proposed structures.

#	k'	Relative intensity*	Proposed compound	Proposed formula	Molar mass (g mol ⁻¹)	Exp. m/z*	Exp. abundance*	Proposed ion	Theoretical m/z	Theoretical abundance	m/z error (ppm)
1	2.6	6.4×10 ⁻⁵	C ₆₀ epoxide ([6,6]C ₆₀ O)	C ₆₀ O	736.6	735.9953	100	[¹² C ₆₀ O] ⁻	735.9955	100	0.27
						736.9988	72	[¹² C ₅₉ ¹³ C ₁ O] ⁻	736.9988	65	0.00
2	3.0	6.6×10 ⁻⁵	Diepoxidized C ₆₀ (<i>cis-I</i> isomer)	C ₆₀ O ₂	752.6	751.9905	100	[¹² C ₆₀ O ₂] ⁻	751.9904	100	0.13
						752.9940	68	[¹² C ₅₉ ¹³ C ₁ O ₂] ⁻	752.9937	65	0.40
3	6.2	3.3×10 ⁻⁵	Diepoxidized C ₆₀	C ₆₀ O ₂	752.6	751.9905	100	[¹² C ₆₀ O ₂] ⁻	751.9904	100	0.13
						752.9941	68	[¹² C ₅₉ ¹³ C ₁ O ₂] ⁻	752.9937	65	0.53
4	3.8	<1.0×10 ⁻⁷	Triepoxidized C ₆₀	C ₆₀ O ₃	768.6	767.9856	100	[¹² C ₆₀ O ₃] ⁻	767.9853	100	0.39
						768.9883	69	[¹² C ₅₉ ¹³ C ₁ O ₃] ⁻	768.9886	65	0.39
5	6.4	5.5×10 ⁻⁵	Triepoxidized C ₆₀ (C _{3v} sym.)	C ₆₀ O ₃	768.6	767.9850	100	[¹² C ₆₀ O ₃] ⁻	767.9853	100	0.39
						768.9884	67	[¹² C ₅₉ ¹³ C ₁ O ₃] ⁻	768.9886	65	0.26
6	10.5	1.4×10 ⁻⁴	Tetraepoxidized C ₆₀	C ₆₀ O ₄	784.6	783.9800	100	[¹² C ₆₀ O ₄] ⁻	783.9802	100	0.26
						784.9834	68	[¹² C ₅₉ ¹³ C ₁ O ₄] ⁻	784.9836	65	0.25
7	7.2	1.3×10 ⁻⁵	C ₆₀ dimer linked by 1 furane-like ring	(C ₆₀) ₂ O	1457	1455.9958	76	[¹² C ₁₂₀ O] ⁻	1455.9955	77	0.21
						1456.9992	100	[¹² C ₁₁₉ ¹³ C ₁ O] ⁻	1456.9988	100	0.27
8	8.2	2.7×10 ⁻⁵	C ₆₀ dimer linked by 2 furane-like rings	(C ₆₀) ₂ O ₂	1473	1471.9888	75	[¹² C ₁₂₀ O ₂] ⁻	1471.9904	77	1.09
						1472.9924	100	[¹² C ₁₁₉ ¹³ C ₁ O ₂] ⁻	1472.9937	100	0.88
9	15.5	9.8×10 ⁻⁶	Mixture of other unresolved dimers	(C ₆₀) ₂ O ₂	1473	1471.9890	72	[¹² C ₁₂₀ O ₂] ⁻	1471.9904	77	0.95
						1472.9933	100	[¹² C ₁₁₉ ¹³ C ₁ O ₂] ⁻	1472.9937	100	0.27
10	19.2	9.9×10 ⁻⁵	Mixture of other unresolved dimers	(C ₆₀) ₂ O ₂	1473	1471.9888	78	[¹² C ₁₂₀ O ₂] ⁻	1471.9904	77	1.09
						1472.9922	100	[¹² C ₁₁₉ ¹³ C ₁ O ₂] ⁻	1472.9937	100	1.02

* Defined as the ratio between the areas of each transformation product peak and that of C₆₀ fullerene after 48 h of agitation in ultrapure water with irradiation.

** Isotopic pattern, defined as the average intensity of all the spectra acquired in the chromatographic peak with an intensity >10 % of the maximum height.

Table 3. Behaviour of the fullerene epoxides in experiments suspended in ultrapure water.

Compound		Experiment with light exposure		Experiment without light exposure	
Formula	k'	Linear range ¹	Slope ² (h ⁻¹)	Linear range ¹	Slope ² (h ⁻¹)
C₆₀O	2.6	0 h to 1.0 h (r=0.90)	2.6×10^{-5}	0 h to 96 h (r=0.93)	7.3×10^{-7}
C₆₀O₂	3.0	0 h to 1.5 h (r=0.94)	1.4×10^{-4}	0 h to 96 h (r=0.91)	9.6×10^{-7}
C₆₀O₂	6.2	0 h to 1.5 h (r=0.98)	9.0×10^{-5}	0 h to 96 h (r=0.91)	1.0×10^{-6}
C₆₀O₃	3.8	0 h to 1.5 h (r=0.98)	5.6×10^{-6}	0 h to 24 h (r=0.91)	8.2×10^{-8}
C₆₀O₃	6.4	0 h to 1.5 h (r=0.98)	4.2×10^{-5}	0 h to 96 h (r=0.97)	7.5×10^{-7}
C₆₀O₄	10.5	0 h to 1.5 h (r=1.00)	1.0×10^{-4}	0 h to 96 h (r=0.94)	2.5×10^{-7}

¹Defined as the interval of time in which the normalized concentration of epoxide evolved linearly, this is, with a Pearson Index >0.90.

²Calculated for comparison purposes as the slope of the linear regression obtained when representing the concentration of epoxide, normalized by the concentration of C₆₀, against the time of exposure.

Figure 1. Extracted Ion Chromatograms of $m/z=720.0005\pm 0.0010$ (a), 735.9954 ± 0.0010 (b), $m/z=751.9905\pm 0.0010$ (c), $m/z=767.9856\pm 0.0010$ (d) and 783.9800 ± 0.0010 (e).

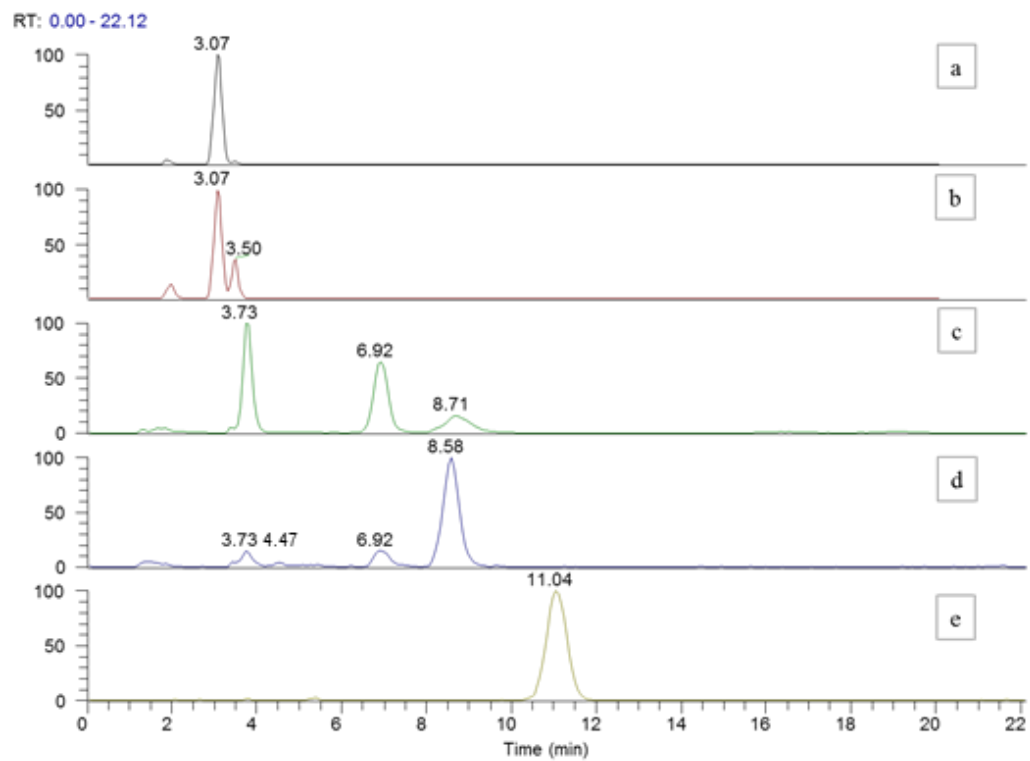


Figure 2. Relative positions of the epoxide functional groups in the eight isomers of diepoxidized fullerene C_{60} . All the regioisomers are produced by the addition of oxygen atoms in [6,6] bonds.

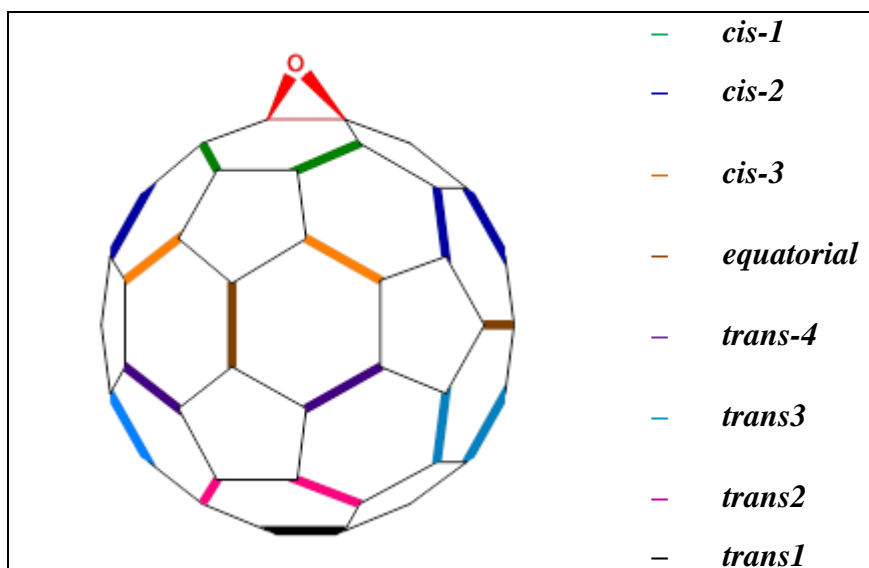
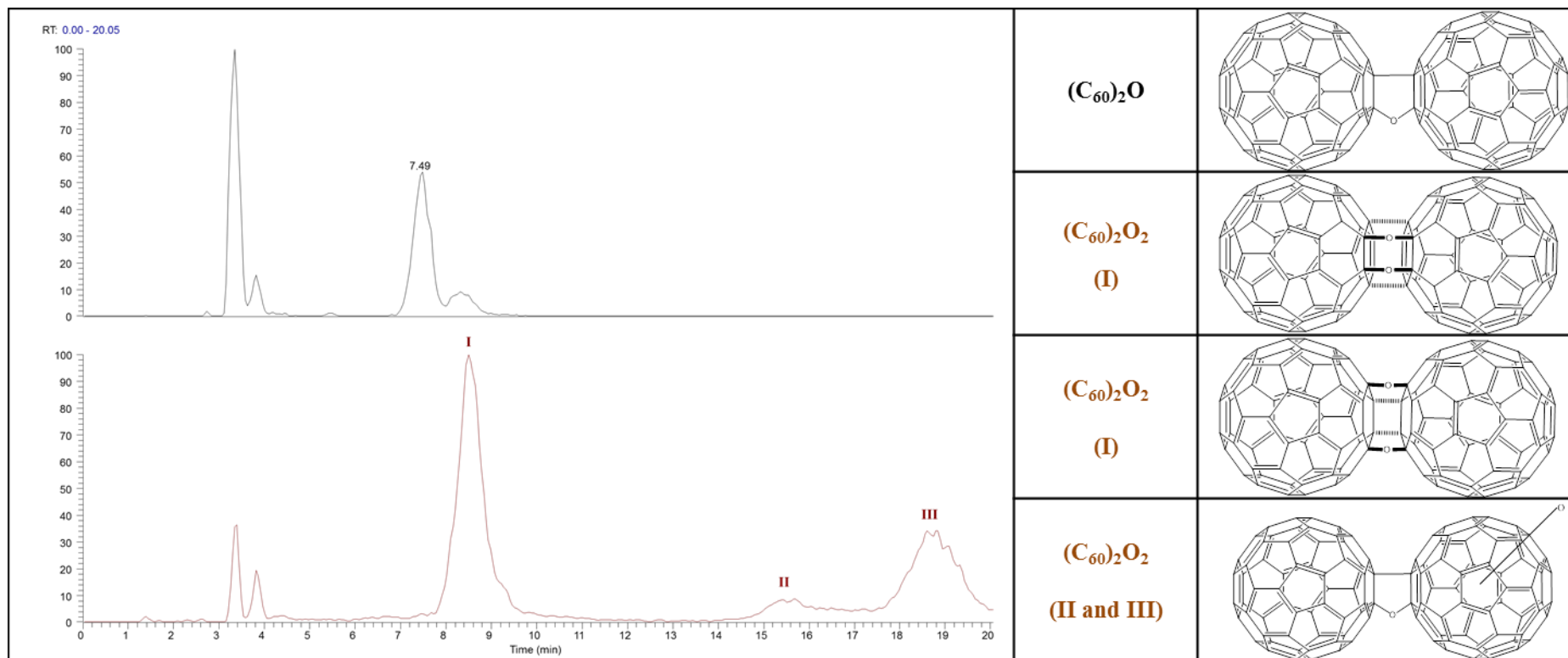
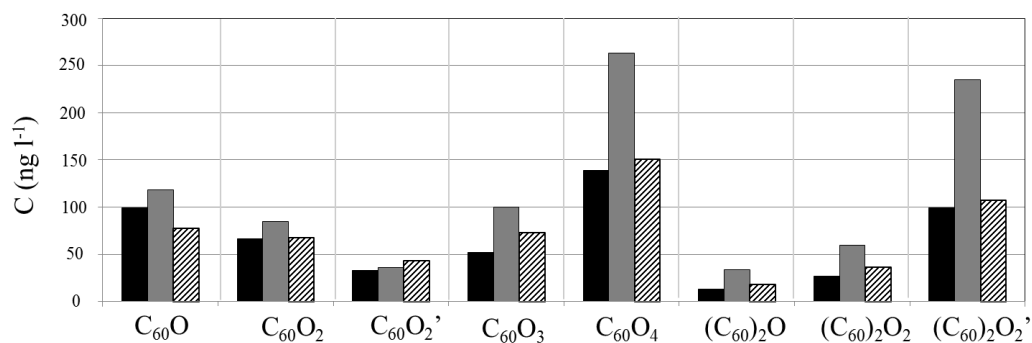


Figure 3. Extracted Ion Chromatogram of $m/z=1455.9958$ (top) and $m/z=1471.9888$ (bottom), corresponding to oxidized and dioxidized fullerene dimers, and their proposed structures.



1 **Figure 4.** Occurrence of degradation products of C_{60} fullerene after 48 hours of simulated
2 sunlight irradiation in ultrapure water (black bars), in artificial freshwater (grey bars) and in
3 artificial seawater (dashed bars). The concentrations of degradation products were estimated
4 semi-quantitatively, because of the absence of commercially available analytical standards,
5 considering that they had the same response factor than C_{60} fullerene.



7

8 **References**

- 9 [1] H.W. Kroto, J.R. Heath, S.C. O'Brien, R.F. Curl, R.E. Smalley, C₆₀: buckminsterfullerene,
10 *Nature* 318(6042) (1985) 162-163.
- 11 [2] S. Vidal, Glycofullerenes: Sweet fullerenes vanquish viruses, *Nat Chem* 8(1) (2016) 4-6.
- 12 [3] R. Bakry, R.M. Vallant, M. Najam-ul-Haq, M. Rainer, Z. Szabo, C.W. Huck, G.K. Bonn,
13 Medicinal applications of fullerenes, *International journal of nanomedicine* 2(4) (2007) 639.
- 14 [4] K. Jinno, K. Yamamoto, J.C. Fetzer, W.R. Biggs, C₆₀ as a stationary phase for microcolumn
15 liquid chromatographic separation of polycyclic aromatic hydrocarbons, *Journal of*
16 *Microcolumn Separations* 4(3) (1992) 187-190.
- 17 [5] R.N. Goyal, V.K. Gupta, N. Bachheti, R.A. Sharma, Electrochemical sensor for the
18 determination of dopamine in presence of high concentration of ascorbic acid using a
19 Fullerene-C₆₀ coated gold electrode, *Electroanalysis* 20(7) (2008) 757-764.
- 20 [6] H. Park, J. Park, A.K.L. Lim, E.H. Anderson, A.P. Alivisatos, P.L. McEuen, Nanomechanical
21 oscillations in a single-C₆₀ transistor, *Nature* 407(6800) (2000) 57-60.
- 22 [7] R. Haddon, A. Perel, R. Morris, T. Palstra, A. Hebard, R. Fleming, C₆₀ thin film transistors,
23 *Applied Physics Letters* 67(1) (1995) 121-123.
- 24 [8] C.J. Brabec, S. Gowrisanker, J.J.M. Halls, D. Laird, S. Jia, S.P. Williams, Polymer-Fullerene
25 Bulk-Heterojunction Solar Cells, *Advanced Materials* 22(34) (2010) 3839-3856.
- 26 [9] B.C. Thompson, J.M.J. Fréchet, Polymer-fullerene composite solar cells, *Angewandte*
27 *Chemie International Edition* 47(1) (2008) 58-77.
- 28 [10] L.T. Lukich, T.E. Duncan, C.M. Lansinger, Use of fullerene carbon in curable rubber
29 compounds, Google Patents, 1998.
- 30 [11] B. Jurkowska, B. Jurkowski, P. Kamrowski, S. Pesetskii, V. Koval, L. Pinchuk, Y.A. Olkhov,
31 Properties of fullerene-containing natural rubber, *Journal of applied polymer science* 100(1)
32 (2006) 390-398.
- 33 [12] T.K. Daly, P.R. Buseck, P. Williams, C.F. Lewis, Fullerenes from a Fulgurite, *Science*
34 259(5101) (1993) 1599-1601.
- 35 [13] L. Becker, J.L. Bada, Fullerenes in Allende meteorite, *Nature* 372 (1994) 507.
- 36 [14] L. Becker, T.E. Bunch, L.J. Allamandola, Higher fullerenes in the Allende meteorite,
37 *Nature* 400(6741) (1999) 227-228.
- 38 [15] D. Heymann, A. Korochantsev, M.A. Nazarov, J. Smit, Search for fullerenes C₆₀ and C₇₀
39 in Cretaceous-Tertiary boundary sediments from Turkmenistan, Kazakhstan, Georgia,
40 Austria, and Denmark, *Cretaceous Research* 17(3) (1996) 367-380.
- 41 [16] L.I. Yanfang, L. Handong, Y.I.N. Hongfu, S.U.N. Jing, C.A.I. Hou'an, R.A.O. Zhu, R.A.N.
42 Fanlin, Determination of Fullerenes (C₆₀/C₇₀) from the Permian-Triassic Boundary in the
43 Meishan Section of South China, *Acta Geologica Sinica - English Edition* 79(1) (2005) 11-15.
- 44 [17] Z. Su, W. Zhou, Y. Zhang, New insight into the soot nanoparticles in a candle flame,
45 *Chemical Communications* 47(16) (2011) 4700-4702.
- 46 [18] A.J. Tiwari, M. Ashraf-Khorassani, L.C. Marr, C₆₀ fullerenes from combustion of
47 common fuels, *Science of the Total Environment* 547 (2016) 254-260.
- 48 [19] E. Emke, J. Sanchis, M. Farre, P. Bäuerlein, P. de Voogt, Determination of several
49 fullerenes in sewage water by LC HR-MS using atmospheric pressure photoionisation,
50 *Environmental Science: Nano* 2(2) (2015) 167-176.

- 51 [20] J. Sanchís, N. Berrojalbiz, G. Caballero, J. Dachs, M. Farré, D. Barceló, Occurrence of
52 Aerosol-Bound Fullerenes in the Mediterranean Sea Atmosphere, *Environmental Science &*
53 *Technology* 46(3) (2012) 1335-1343.
- 54 [21] J. Sanchís, C. Bosch-Orea, M. Farré, D. Barceló, Nanoparticle tracking analysis
55 characterisation and parts-per-quadrillion determination of fullerenes in river samples from
56 Barcelona catchment area, *Analytical and bioanalytical chemistry* 407(15) (2015) 4261-4275.
- 57 [22] J. Sanchís, D. Božović, N.A. Al-Harbi, L.F. Silva, M. Farré, D. Barceló, Quantitative trace
58 analysis of fullerenes in river sediment from Spain and soils from Saudi Arabia, *Analytical*
59 *and bioanalytical chemistry* 405(18) (2013) 5915-5923.
- 60 [23] A. Astefanei, O. Núñez, M.T. Galceran, Analysis of C₆₀-fullerene derivatives and pristine
61 fullerenes in environmental samples by ultrahigh performance liquid chromatography-
62 atmospheric pressure photoionization-mass spectrometry, *Journal of Chromatography A*
63 1365 (2014) 61-71.
- 64 [24] Ó. Núñez, H. Gallart-Ayala, C.P.B. Martins, E. Moyano, M.T. Galceran, Atmospheric
65 Pressure Photoionization Mass Spectrometry of Fullerenes, *Analytical Chemistry* 84(12)
66 (2012) 5316-5326.
- 67 [25] S. Utsunomiya, K.A. Jensen, G.J. Keeler, R.C. Ewing, Uraninite and Fullerene in
68 Atmospheric Particulates, *Environmental Science & Technology* 36(23) (2002) 4943-4947.
- 69 [26] T. Laitinen, T. Petäjä, J. Backman, K. Hartonen, H. Junninen, J. Ruiz-Jiménez, D.
70 Worsnop, M. Kulmala, M.-L. Riekkola, Carbon clusters in 50 nm urban air aerosol particles
71 quantified by laser desorption-ionization aerosol mass spectrometer, *International Journal*
72 *of Mass Spectrometry* 358(0) (2014) 17-24.
- 73 [27] J. Jehlička, O. Frank, V. Hamplová, Z. Pokorná, L. Juha, Z. Boháček, Z. Weishauptová,
74 Low extraction recovery of fullerene from carbonaceous geological materials spiked with
75 C₆₀, *Carbon* 43(9) (2005) 1909-1917.
- 76 [28] J. Sanchís, L.F.S. Oliveira, F.B. de Leão, M. Farré, D. Barceló, Liquid chromatography-
77 atmospheric pressure photoionization-Orbitrap analysis of fullerene aggregates on surface
78 soils and river sediments from Santa Catarina (Brazil), *Science of the Total Environment* 505
79 (2015) 172-179.
- 80 [29] A. Astefanei, O. Núñez, M.T. Galceran, Characterisation and determination of
81 fullerenes: A critical review, *Analytica chimica acta* 882 (2015) 1-21.
- 82 [30] C.T. Jafvert, P.P. Kulkarni, Buckminsterfullerene's (C₆₀) Octanol-Water Partition
83 Coefficient (K_{ow}) and Aqueous Solubility, *Environmental Science & Technology* 42(16)
84 (2008) 5945-5950.
- 85 [31] M. Farré, S. Pérez, K. Gajda-Schranz, V. Osorio, L. Kantiani, A. Ginebreda, D. Barceló,
86 First determination of C₆₀ and C₇₀ fullerenes and N-methylfulleropyrrolidine C₆₀ on the
87 suspended material of wastewater effluents by liquid chromatography hybrid quadrupole
88 linear ion trap tandem mass spectrometry, *Journal of Hydrology(Amsterdam)* 383(1-2)
89 (2010) 44-51.
- 90 [32] S. Deguchi, R.G. Alargova, K. Tsujii, Stable Dispersions of Fullerenes, C₆₀ and C₇₀, in
91 Water. Preparation and Characterization, *Langmuir* 17(19) (2001) 6013-6017.
- 92 [33] G.V. Andrievsky, V.K. Klochkov, A.B. Bordyuh, G.I. Dovbeshko, Comparative analysis of
93 two aqueous-colloidal solutions of C₆₀ fullerene with help of FTIR reflectance and UV-Vis
94 spectroscopy, *Chemical Physics Letters* 364(1-2) (2002) 8-17.
- 95 [34] B. Derjaguin, L. Landau, Theory of the stability of strongly charged lyophobic sols and of
96 the adhesion of strongly charged particles in solutions of electrolytes, *Acta physicochim.*
97 *URSS* 14(6) (1941) 633-662.

- 98 [35] K.L. Chen, M. Elimelech, Influence of humic acid on the aggregation kinetics of fullerene
99 (C₆₀) nanoparticles in monovalent and divalent electrolyte solutions, *Journal of Colloid and*
100 *Interface Science* 309(1) (2007) 126-134.
- 101 [36] E.J.W. Verwey, J.T.G. Overbeek, J.T.G. Overbeek, *Theory of the stability of lyophobic*
102 *colloids*, Courier Corporation 1999.
- 103 [37] Q. Li, B. Xie, Y.S. Hwang, Y. Xu, Kinetics of C₆₀ Fullerene Dispersion in Water Enhanced
104 by Natural Organic Matter and Sunlight, *Environmental Science & Technology* 43(10) (2009)
105 3574-3579.
- 106 [38] C.W. Isaacson, D.C. Bouchard, Effects of Humic Acid and Sunlight on the Generation and
107 Aggregation State of Aqu/C₆₀ Nanoparticles, *Environmental Science & Technology* 44(23)
108 (2010) 8971-8976.
- 109 [39] J.W. Arbogast, A.P. Darmanyan, C.S. Foote, F.N. Diederich, R. Whetten, Y. Rubin, M.M.
110 Alvarez, S.J. Anz, Photophysical properties of sixty atom carbon molecule (C₆₀), *The Journal*
111 *of Physical Chemistry* 95(1) (1991) 11-12.
- 112 [40] J. Lee, J.D. Fortner, J.B. Hughes, J.-H. Kim, Photochemical Production of Reactive Oxygen
113 Species by C₆₀ in the Aqueous Phase During UV Irradiation, *Environmental Science &*
114 *Technology* 41(7) (2007) 2529-2535.
- 115 [41] J. Lee, Y. Yamakoshi, J.B. Hughes, J.-H. Kim, Mechanism of C₆₀ photoreactivity in water:
116 Fate of triplet state and radical anion and production of reactive oxygen species,
117 *Environmental science & technology* 42(9) (2008) 3459-3464.
- 118 [42] W.-C. Hou, C.T. Jafvert, Photochemical Transformation of Aqueous C₆₀ Clusters in
119 Sunlight, *Environmental Science & Technology* 43(2) (2008) 362-367.
- 120 [43] W.-C. Hou, C.T. Jafvert, Photochemistry of aqueous C₆₀ clusters: evidence of ¹O₂
121 formation and its role in mediating C₆₀ phototransformation, *Environmental science &*
122 *technology* 43(14) (2009) 5257-5262.
- 123 [44] W.-C. Hou, L. Kong, K.A. Wepasnick, R.G. Zepp, D.H. Fairbrother, C.T. Jafvert,
124 Photochemistry of Aqueous C₆₀ Clusters: Wavelength Dependency and Product
125 Characterization, *Environmental Science & Technology* 44(21) (2010) 8121-8127.
- 126 [45] C. Taliani, G. Ruani, R. Zamboni, R. Danieli, S. Rossini, V. Denisov, V. Burlakov, F. Negri,
127 G. Orlandi, F. Zerbetto, Light-induced oxygen incision of C₆₀, *Journal of the Chemical*
128 *Society, Chemical Communications* (3) (1993) 220-222.
- 129 [46] R. Gelca, K. Surowiec, T.A. Anderson, S.B. Cox, Photolytic breakdown of fullerene C₆₀
130 cages in an aqueous suspension, *Journal of nanoscience and nanotechnology* 11(2) (2011)
131 1225-1229.
- 132 [47] D. Heymann, S.M. Bachilo, R.B. Weisman, F. Cataldo, R.H. Fokkens, N.M.M. Nibbering,
133 R.D. Vis, L.P.F. Chibante, C₆₀O₃, a Fullerene Ozonide: Synthesis and Dissociation to C₆₀O
134 and O₂, *Journal of the American Chemical Society* 122(46) (2000) 11473-11479.
- 135 [48] B.S. Murdianti, J.T. Damron, M.E. Hilburn, R.D. Maples, R.S. Hikkaduwa Koralege, S.I.
136 Kuriyavar, K.D. Ausman, C₆₀ oxide as a key component of aqueous C₆₀ colloidal
137 suspensions, *Environmental science & technology* 46(14) (2012) 7446-7453.
- 138 [49] A.J. Tiwari, J.R. Morris, E.P. Vejerano, M.F. Hochella Jr, L.C. Marr, Oxidation of C₆₀
139 aerosols by atmospherically relevant levels of O₃, *Environmental science & technology* 48(5)
140 (2014) 2706-2714.
- 141 [50] A. Carboni, R. Helmus, J.R. Parsons, K. Kalbitz, P. de Voegt, Incubation of solid state C₆₀
142 fullerene under UV irradiation mimicking environmentally relevant conditions,
143 *Chemosphere* 175 (2017) 1-7.

- 144 [51] H. Mashayekhi, S. Ghosh, P. Du, B. Xing, Effect of natural organic matter on aggregation
145 behavior of C60 fullerene in water, *Journal of Colloid and Interface Science* 374(1) (2012)
146 111-117.
- 147 [52] K.L. Chen, M. Elimelech, Interaction of Fullerene (C60) Nanoparticles with Humic Acid
148 and Alginate Coated Silica Surfaces: Measurements, Mechanisms, and Environmental
149 Implications, *Environmental Science & Technology* 42(20) (2008) 7607-7614.
- 150 [53] D.R. Kester, I.W. Duedall, D.N. Connors, R.M. Pytkowicz, Preparation of artificial
151 seawater, *Limnol. Oceanogr* 12(1) (1967) 176-179.
- 152 [54] D.L. Lipschitz, W.C. Michel, Amino acid odorants stimulate microvillar sensory neurons,
153 *Chemical senses* 27(3) (2002) 277-286.
- 154 [55] A. Hirsch, *The chemistry of the fullerenes*, Wiley Online Library 1994.
- 155 [56] Y. Elemes, S.K. Silverman, C. Sheu, M. Kao, C.S. Foote, M.M. Alvarez, R.L. Whetten,
156 Reaction of C60 with Dimethyldioxirane—Formation of an Epoxide and a 1, 3-Dioxolane
157 Derivative, *Angewandte Chemie International Edition in English* 31(3) (1992) 351-353.
- 158 [57] S. Patai, *The chemistry of peroxides*, John Wiley & Sons 2015.
- 159 [58] R. Dattani, K.F. Gibson, S. Few, A.J. Borg, P.A. DiMaggio, J. Nelson, S.G. Kazarian, J.T.
160 Cabral, Fullerene oxidation and clustering in solution induced by light, *Journal of colloid and*
161 *interface science* 446 (2015) 24-30.
- 162 [59] A.L. Balch, D.A. Costa, B.C. Noll, M.M. Olmstead, Oxidation of buckminsterfullerene
163 with m-chloroperoxybenzoic acid. Characterization of a Cs isomer of the diepoxide C60O2,
164 *Journal of the American Chemical Society* 117(35) (1995) 8926-8932.
- 165 [60] Y. Tajima, K. Takeshi, Y. Shigemitsu, Y. Numata, Chemistry of fullerene epoxides:
166 Synthesis, structure, and nucleophilic substitution-addition reactivity, *Molecules* 17(6)
167 (2012) 6395-6414.
- 168 [61] J.-P. Deng, C.-Y. Mou, C.-C. Han, Electrospray and laser desorption ionization studies of
169 C60O and isomers of C60O2, *The Journal of Physical Chemistry* 99(41) (1995) 14907-14910.
- 170 [62] J. Feng, A. Ren, W. Tian, M. Ge, Z. Li, C. Sun, X. Zheng, M.C. Zerner, Theoretical studies
171 on the structure and electronic spectra of some isomeric fullerene derivatives C60On (n= 2,
172 3), *International Journal of Quantum Chemistry* 76(1) (2000) 23-43.
- 173 [63] D. Heymann, S.M. Bachilo, R.B. Weisman, F. Cataldo, R.H. Fokkens, N.M. Nibbering, R.D.
174 Vis, L.F. Chibante, C60O3, a fullerene ozonide: synthesis and dissociation to C60O and O2,
175 *Journal of the American Chemical Society* 122(46) (2000) 11473-11479.
- 176 [64] Y. Tajima, K. Takeuchi, Discovery of C60O3 Isomer Having C_{3v} Symmetry, *The Journal*
177 *of organic chemistry* 67(5) (2002) 1696-1698.
- 178 [65] M. Manoharan, Predicting efficient C60 epoxidation and viable multiple oxide
179 formation by theoretical study, *The Journal of organic chemistry* 65(4) (2000) 1093-1098.
- 180 [66] R. Bulgakov, E.Y. Nevyadovskii, A. Belyaeva, M. Golikova, Z. Ushakova, Y.G.
181 Ponomareva, U. Dzhemilev, S. Razumovskii, F. Valyamova, Water-soluble polyketones and
182 esters as the main stable products of ozonolysis of fullerene C60 solutions, *Russian chemical*
183 *bulletin* 53(1) (2004) 148-159.
- 184 [67] N. Xin, X. Yang, Z. Zhou, J. Zhang, S. Zhang, L. Gan, Synthesis of C60(O)3: An open-cage
185 fullerene with a ketolactone moiety on the orifice, *The Journal of organic chemistry* 78(3)
186 (2013) 1157-1162.
- 187 [68] S. Lebedkin, S. Ballenweg, J. Gross, R. Taylor, W. Krätschmer, Synthesis of C₁₂₀O: A new
188 dimeric [60] fullerene derivative, *Tetrahedron letters* 36(28) (1995) 4971-4974.

- 189 [69] A. Gromov, S. Lebedkin, S. Ballenweg, A.G. Avent, R. Taylor, W. Krätschmer, C₁₂₀O₂: The
190 first [60] fullerene dimer with cages bis-linked by furanoid bridges, *Chemical*
191 *Communications* (2) (1997) 209-210.
- 192 [70] R. Taylor, M.P. Barrow, T. Drewello, C 60 degrades to C 120 O, *Chemical*
193 *Communications* (22) (1998) 2497-2498.
- 194 [71] M. Sillion, A. Dascalu, M. Pinteala, B.C. Simionescu, C. Ungurenasu, A study on
195 electrospray mass spectrometry of fulleranol C₆₀(OH)₂₄, *Beilstein journal of organic*
196 *chemistry* 9(1) (2013) 1285-1295.
- 197 [72] J. Labille, A. Masion, F. Ziarelli, J. Rose, J. Brant, F. Villiéras, M. Pelletier, D. Borschneck,
198 M.R. Wiesner, J.-Y. Bottero, Hydration and Dispersion of C60 in Aqueous Systems: The
199 Nature of Water–Fullerene Interactions, *Langmuir* 25(19) (2009) 11232-11235.
- 200 [73] Y.S. Hwang, Q. Li, Characterizing Photochemical Transformation of Aqueous nC₆₀ under
201 Environmentally Relevant Conditions, *Environmental Science & Technology* 44(8) (2010)
202 3008-3013.
- 203 [74] J. Brant, H. Lecoanet, M.R. Wiesner, Aggregation and Deposition Characteristics of
204 Fullerene Nanoparticles in Aqueous Systems, *Journal of Nanoparticle Research* 7(4) (2005)
205 545-553.
- 206 [75] X. Qu, P.J. Alvarez, Q. Li, Impact of sunlight and humic acid on the deposition kinetics of
207 aqueous fullerene nanoparticles (nC60), *Environmental science & technology* 46(24) (2012)
208 13455-13462.
- 209 [76] K. Polewski, D. Sławińska, J. Sławiński, A. Pawlak, The effect of UV and visible light
210 radiation on natural humic acid: EPR spectral and kinetic studies, *Geoderma* 126(3–4) (2005)
211 291-299.
- 212 [77] M. Kah, X. Zhang, T. Hofmann, Sorption behavior of carbon nanotubes: Changes
213 induced by functionalization, sonication and natural organic matter, *Science of The Total*
214 *Environment* 497-498(0) (2014) 133-138.
- 215 [78] H.S. Thorsten Hüffer, Melanie Kah, Thilo Hofmann, Sorption of substituted aromatic
216 hydrocarbons by fullerenes - Influence of functionalization on molecular interactions, Poster
217 presentation at the SETAC Europe 26th Annual Meeting (Nantes, France, 2016) (2016).
- 218 [79] K. Gai, B. Shi, X. Yan, D. Wang, Effect of dispersion on adsorption of atrazine by aqueous
219 suspensions of fullerenes, *Environmental science & technology* 45(14) (2011) 5959-5965.
- 220 [80] T. Hüffer, M. Kah, T. Hofmann, T.C. Schmidt, How redox conditions and irradiation
221 affect sorption of PAHs by dispersed fullerenes (nC60), *Environmental science & technology*
222 47(13) (2013) 6935-6942.
- 223 [81] T.D. Berry, A.P. Clavijo, Y. Zhao, C.T. Jafvert, R.F. Turco, T.R. Filley, Soil microbial
224 response to photo-degraded C60 fullerenes, *Environmental Pollution* 211 (2016) 338-345.
- 225 [82] T.M. Sakellarides, M.G. Siskos, T.A. Albanis, Photodegradation of selected
226 organophosphorus insecticides under sunlight in different natural waters and soils,
227 *International Journal of Environmental & Analytical Chemistry* 83(1) (2003) 33-50.

229

230

SUPPLEMENTARY INFORMATION

231

232

233

234 **Transformation of C₆₀ fullerene aggregates suspended and weathered under realistic**

235

environmental conditions

236 Josep Sanchís^{1,†}, Yann Aminot^{2,†}, Esteban Abad¹, Damià Barceló^{1,3}, James W. Readman²,

237

Marinella Farré^{1,*}

238

239 ¹ Water and Soil Quality Research Group, Institute of Environmental Assessment and Water
240 Research (IDAEA-CSIC), C/Jordi Girona, 18-26, 08034, Barcelona, Catalonia, Spain.

241 ² Plymouth University, Plymouth, England, UK.

242 ³ Catalan Institute of Water Research (ICRA), C/ Emili Grahit, 101, 17003 Girona, Catalonia,
243 Spain.

244

245

246

247 [†] Both authors contributed equally to this work.

248

* *Corresponding author:* mfuqam@cid.csic.es

249

250 **Text S1. Extraction optimization**

251 Optimization: A simple one-step liquid-liquid extraction method was optimized. Three C₆₀
252 suspensions were prepared at ~1.0 mg l⁻¹ in three different water matrices (UPW, AFW and
253 ASW) and weathered under ambient sunlight irradiation during 24 h with constant stirring.
254 Five extraction solvents were tested: toluene, *o*-dichlorobenzene, ethyl acetate,
255 dichloromethane and the water-insoluble ionic liquid [BMIM][PF₆].

256 Results: Based on the amount of C₆₀ and C₆₀O₂ recovered, the performance of the tested
257 solvents ranked as follows: toluene > *o*-dichlorobenzene > dichloromethane > ethyl acetate >
258 [BMIM][PF₆] (see **Figure S1**). Toluene was the optimal extraction solvent. The three non-
259 aromatic compounds (the ionic liquid, dichloromethane and ethyl acetate) showed the lowest
260 recovery yields, always lower than 4 %. In addition, the peak shape worsened significantly
261 when injecting dichloromethane and [BMIM][PF₆] extracts, probably because of the low
262 diffusion of these solvents into the mobile phase. On the contrary, *o*-dichlorobenzene and,
263 especially, toluene, offered good recoveries.

264 In addition, as can be seen in **Figure S1**, the extraction recovery was slightly dependent on
265 the ionic strength of the matrix, as it has been reported in other works which recommend
266 salting out the water sample to optimize the extraction of fullerenes [1].

267

268 **Text S2: Chromatographic optimization**

269 The formation of fullerene adducts was first reported by van Wezel *et al.* (2011) [2]. The
270 simultaneous analysis of fullerene C₆₀ and their transformation products is challenging
271 because oxygenated adducts produce signals with the same m/z than the molecular ions of
272 degradation products generated under environmental conditions. In addition, C₆₀O_x molecules
273 are fragmented in the ionisation source losing oxygen atoms. Therefore, C₆₀ and their
274 oxidized transformation products have a common series of isobaric signals that can
275 potentially interfere with each other if they are not correctly separated by the
276 chromatographic step (see **Table S1**).

277 A toluene extract of C₆₀, suspended in UPW and weathered as described in **Text S1**, was used
278 for the chromatographic optimisation. The separation between the parent C₆₀ fullerene and
279 the generated transformation products C₆₀O and C₆₀O₂ was optimised.

280 Four LC columns were tested:

- 281 ▪ A Luna® C18 column (length, 15.0 cm; diameter, 2 mm; particle size, 5 µm; pore
282 size, 100 Å) from Phenomenex, Torrance, CA, USA;
- 283 ▪ a HILIC column (length, 15.0 cm; diameter, 2 mm; particle size, 3 µm; pore size, 200
284 Å) from Phenomenex, Torrance, CA, USA;
- 285 ▪ a Cosmosil Buckyprep D column (length, 15.0 cm; diameter, 2 mm; particle size, 5
286 µm; pore size, ~120 Å) from Nacalai Tesque Inc., Kyoto, Japan; and
- 287 ▪ a Cosmosil Buckyprep column (length, 15.0 cm; diameter, 2 mm; particle size, 5 µm;
288 pore size, ~120 Å) from Nacalai Tesque Inc., Kyoto, Japan.

289 Tests with C18 columns using isocratic mobile phases consisting in toluene:methanol (1:1)
290 and toluene:acetonitrile (1:1) showed no separation of these three peaks. Therefore, other
291 columns were tested.

292 A Luna® HILIC column was also tested. Early tests with H₂O:MeOH and H₂O:ACN
293 gradients were inadequate, since toluene is mandatory for the elution of fullerenes and their
294 oxidized derivatives. Toluene was introduced in tertiary mobile phases of

295 methanol:water:toluene (ratios of 80:15:5, 80:10:10 and 80:5:15). Poor results were obtained
296 because of the high retention of fullerene to the column in these conditions.

297 Non-aqueous HILIC chromatography was employed using methanol and toluene as mobile
298 phases at ratios close to 1:1. Although these conditions offered gaussian peaks with adequate
299 retention factors ($k' \approx 3$, similarly than with conventional non-aqueous reverse phase
300 chromatography with C18 columns), the three compounds, C_{60} , $C_{60}O$ and $C_{60}O_2$, could not be
301 separated.

302 The performance of two columns especially designed for the separation of fullerenes was
303 assessed: A Cosmosil Buckyrep D and a Cosmosil Buckyrep column, with nitrocarbazoil
304 and pyrenylpropyl groups respectively.

305 The Cosmosil Buckyrep D column contains a stationary phases end-capped with
306 nitrocarbazoil groups, especially indicated for the retention of fullerenes with engineered
307 functional group. Isocratic chromatographic programs were tested with toluene:methanol and
308 toluene:hexane at solvent ratios 100:0, 90:10, 80:20, 70:30 and 60:40. In tests with
309 toluene:methanol, when increasing the amount of methanol, the retention time of the
310 compounds decreased and so did their retention factor, from $k'(C_{60})=0.29$ and $k'(C_{60}O_2)=0.99$
311 at 100 % of toluene to $k'(C_{60})=0.01$ and $k'(C_{60}O_2)=0.15$ at 40 % of methanol. In tests with
312 toluene:hexane, the opposite trend was observed and the retention increased when increasing
313 the percentage of hexane. The retention of the analytes increased up to $k'(C_{60})=0.96$ and
314 $k'(C_{60}O_2)=2.9$ at 40 % of hexane.

315 Despite of the good retention and of the Gaussian shape of the peaks, poor chromatographic
316 selectivity was obtained for C_{60} and $C_{60}O$. Both peaks overlapped in all the tested conditions,
317 with an optimal resolution of only 0.12. In tests with toluene:hexane, $C_{60}O_2$ and $C_{60}O$ showed
318 a better selectivity than in tests with toluene:methanol, but the width of the peaks was too
319 large to ensure good chromatographic resolution (R_s): $R_s(C_{60}O, C_{60}O_2)=0.56$ at 20 % of
320 hexane and $R_s(C_{60}O, C_{60}O_2)=0.68$ at 30 % of hexane.

321 Therefore, it was concluded that Buckyrep-D was not an adequate column for the
322 determination of the oxygenated photodegradation products of C_{60} .

323 In constrast, the Buckyrep column showed a good performance and it was finally selected as
324 the optimal column. The best chromatographic separation was observed with 10 % of
325 methanol in the mobile phase (see **Figure S2**). At higher percentages of methanol, higher

326 retention factors (k') were observed for all the compounds and the chromatographic
327 selectivity of C_{60} , $C_{60}O$ and $C_{60}O_2$ improved accordingly, but the widening of the peaks and
328 the subsequent loss of sensitivity prevented the use of methanol percentages higher than 10
329 %. The loss of sensitivity was related to the widening of the chromatographic peak and to the
330 reduction in ionisation efficiency in the APPI source, as toluene acts as a dopant.

331 The pH of the mobile phase was modified by adding formic acid contents of 0.01 % and 0.1
332 % in the methanol. No significant changes were observed in the chromatographic
333 performance, so the mobile phase was not acidified.

334 Finally, the temperature of the column oven was optimized with better results obtained at
335 $T=30$ °C (see **Figure S3**).

336

337 **Text S3: Mass spectrometry optimization**

338 Preliminary experiments with a heated electrospray (H-ESI) source, an atmospheric pressure
339 chemical ionisation (APCI) source and an APPI source showed that APPI system is the
340 optimal, not only for the analysis of pristine fullerenes (as previously reported [3-5]), but also
341 for ionising the transformation products that were studied in the present work.

342 High S-lens values favoured the sensitivity of the method, so it was set at 90 % (see **Figure**
343 **S4**). High temperatures did not favour the ionisation of the compounds, so the capillary
344 temperature was kept at 300 °C and the probe was adjusted at 400 C. Finally, intermediate
345 gas flows, i.e. sheath gas=40 a.u. and auxiliary gas=25 a.u, were the optimal ones. The spare
346 gas was maintained at 1 a.u. in all the experiments.

347 In these conditions, the ionisation of C₆₀ fullerene resulted in several relevant source adducts.
348 Their identity and relative intensities are listed in **Table S2**.

349

350 Text S4: Precautions and safety considerations

351 During samples manipulation and extraction their exposure to ambient air and light was
352 minimized to avoid undesired and uncontrolled degradation of nC_{60} . Toluene extracts were
353 analysed immediately when possible or stored in amber glass vials at $-80\text{ }^{\circ}\text{C}$ until their
354 instrumental analysis, within 12 hours.

355 Plastic material was avoided during the whole experimental work in order to avoid adsorption
356 of fullerene aggregates. Instead, glass, quartz and steel instrumentation was employed.
357 Potential carry-over and cross-contamination were circumvented by rinsing glass and quartz
358 material, before and after using it, with toluene, ethanol and acetone. Glass and quartz
359 material was heated at $400\text{ }^{\circ}\text{C}$ overnight.

360 In order to minimize health risks, samples extraction and manipulation of organic solvents
361 was carried out under extracting fume. The LC-MS system was installed inside a home-made
362 extracting cabin in order to avoid analysts' exposure to toluene vapour from the
363 chromatographic system and the ionisation source.

364

365 **Text S5. Data treatment: necessity to normalize by the concentration of C₆₀ in each**
 366 **time.**

367 A general scheme of all the processes that happened simultaneously during the stirring and
 368 weathering of the aggregates is presented in **Figure S9**, considering (i) those non-suspended
 369 aggregates that are present in the air-water interphase, referred to as $(C_{60})_{suspended}$ and
 370 $(TP)_{suspended}$; (ii) the truly suspended aggregates that are present in the bulk solution, referred
 371 to as $(C_{60})_{suspended}$ and $(TP)_{suspended}$; and (iii) those aggregates that have precipitated or were
 372 stuck on the glass walls, referred to as $(C_{60})_{precip}$ and $(TP)_{precip}$. The following assumptions
 373 were made:

- 374 ▪ Since the degradation experiments were under a constant agitation, $k_{prep.1}$ and $k_{prep.2}$
 375 were considered negligible. Subsequently, k_3 was irrelevant and $[(C_{60})_{precip}]$ and
 376 $[(TP)_{precip}]$ could be considered negligible.
- 377 ▪ Since the concentration of the other species involved in the reactions (presumably ¹O₂,
 378 O₃, and H₂O) was significantly higher than that of C₆₀ and their degradation products,
 379 their concentrations could be considered constant and k_1 and k_2 could be considered
 380 equivalent (k_{degrad}).
- 381 ▪ Since C₆₀ fullerene and their transformation products were expected to aggregate
 382 together, $k_{susp.1}$ and $k_{susp.2}$ were assumed to be equivalent (k_{susp}). k_{susp} was not
 383 necessarily constant through the reaction, since the solubility of the aggregate
 384 increases accordingly with the concentration of oxidized transformation products.

385 The aliquots analysed by LC-MS were taken from the bulk solution, so only $(C_{60})_{suspended}$ and
 386 $(TP)_{suspended}$ were analysed. Both were decisively affected by k_{susp} , so in order to study the
 387 kinetics of degradation circumventing the interference of the kinetic of solubilisation, the
 388 concentrations of transformation products were normalised by the concentration of C₆₀
 389 fullerene at each sampling point. This concentration of C₆₀ in the bulk solution evolved
 390 through time in a non-trivial way and the maximum concentration of C₆₀ was usually
 391 obtained after 12 h~24 h.

392

393 **Table S1.** Intensity of oxygen adducts and “fullerene-like” in-source fragments, normalised
 394 by the intensity of the molecular radical ion (in bold).

	$[\text{C}_{60}]^{\cdot-}$	$[\text{C}_{60}\text{O}]^{\cdot-}$	$[\text{C}_{60}\text{O}_2]^{\cdot-}$	$[\text{C}_{60}\text{O}_3]^{\cdot-}$	$[\text{C}_{60}\text{O}_4]^{\cdot-}$
	m/z=720.0005	m/z=735.9954	m/z=751.9904	m/z=767.9852	m/z=783.9802
C₆₀	1.0	0.019	0.0005	0.0002	<0.0001
C₆₀O (<i>k'</i> =3.0)	4.1	1.0	0.02	0.01	<0.0001
C₆₀O₂ (<i>k'</i> =3.8)	2.1	0.13	1.0	0.07	0.06

395

396

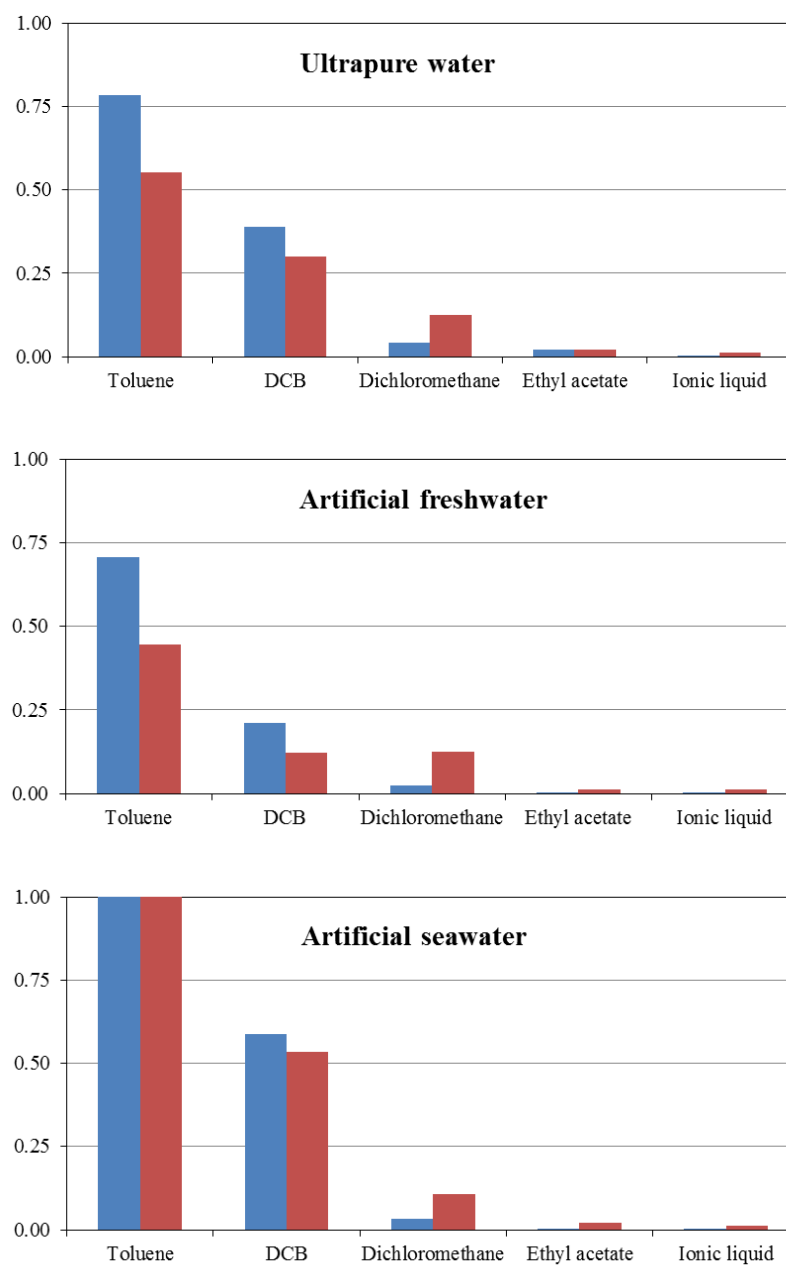
397 **Table S2.** List of adducts and their relative intensities, obtained when analysing a fresh
 398 standard of C₆₀ fullerene in the optimal MS conditions. Experimental m/z presented an error
 399 smaller than 1.5 ppm in all the cases.

	m/z	Adduct	Intensity (%)	Comment
1	721.0084	[C ₆₀ H] ^{·-}	3.5	Proton adduct. Has overlapping with the [¹² C ₅₉ ¹³ C] ^{·-} signal.
2	735.9954	[C ₆₀ O] ^{·-}	1.9	Monoxidized adduct.
3	737.0033	[C ₆₀ OH] ^{·-}	0.47	Hydroxyl adduct. Has overlapping with the [¹² C ₅₉ ¹³ C O] ^{·-} signal.
4	738.0111	[C ₆₀ OH ₂] ^{·-}	0.093	Water adduct (or C ₆₀ +OH+H adduct). Has overlapping with the [¹² C ₅₉ ¹³ C OH] ^{·-} signal.
5	751.9904	[C ₆₀ O ₂] ^{·-}	0.050	Dioxidized adduct.
6	752.9982	[C ₆₀ O ₂ H] ^{·-}	0.75	Overlapping with the [¹² C ₅₉ ¹³ C O ₂] ^{·-} signal.
7	767.9852	[C ₆₀ O ₃] ^{·-}	0.017	Three-fold-oxidized adduct.
8	812.0631	[C ₆₀ C ₇ H ₈] ^{·-}	2.5	Toluene adduct (from the mobile phase)
9	751.0189	[C ₆₀ OCH ₃] ^{·-}	0.021	Methanol adduct (from the mobile phase).
10	844.0893	[C ₆₀ C ₇ H ₈ CH ₃ OH] ^{·-}	0.24	Toluene and methanol adduct (from the mobile phase)
11	720.5022	[C ₆₀ C ₆₀] ^{·2-}	0.0054	Dimer, only observed with double charge.
12	720.3350	[C ₆₀ C ₆₀ C ₆₀] ^{·3-}	0.0012	Trimer, only observed with triple charge.

400

401

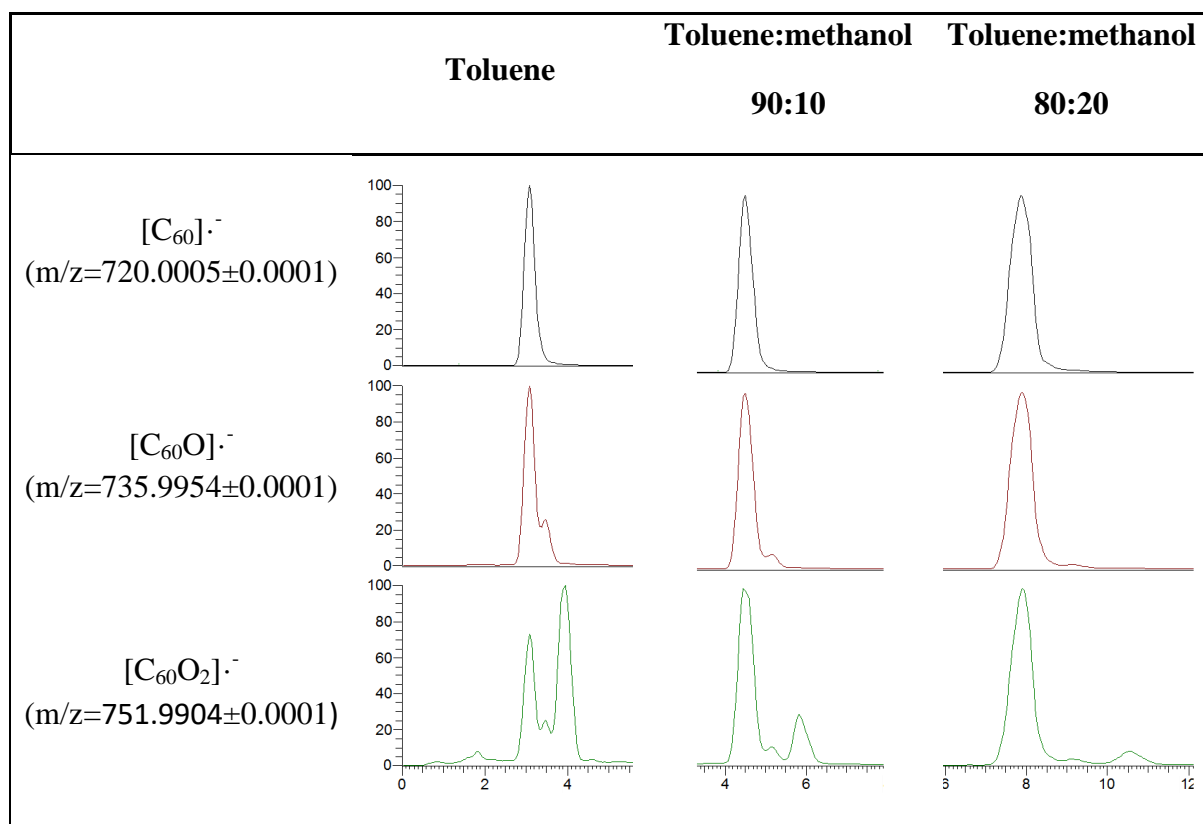
402 **Figure S1.** Extraction of C_{60} and $C_{60}O_2$ with the different tested solvents in the three studied
403 matrixes: ultrapure water, artificial freshwater and artificial seawater.



404

405

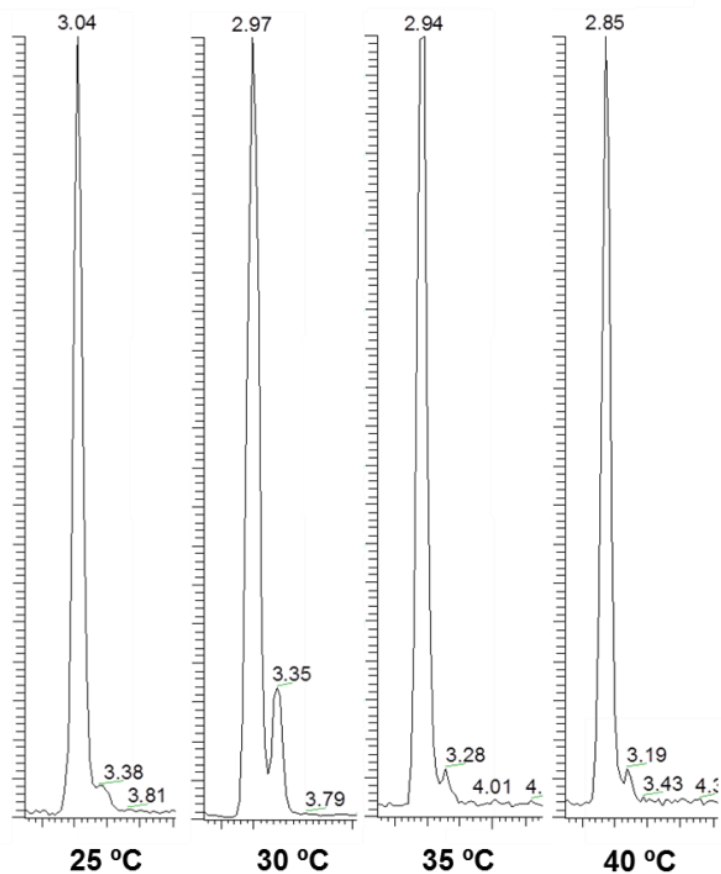
406 **Figure S2.** Separation of C_{60} , $C_{60}O$ and $C_{60}O_2$ in a Buckyprep column, using isocratic mobile
407 phases containing 0 %, 10 % and 20 % of methanol.



408

409

410 **Figure S3.** Extracted ion chromatograms ($m/z=720.0005\pm 0.0001$) showing the
411 chromatographic peaks of C_{60} and its transformation product $C_{60}O$ in a toluene extract.
412 Chromatographic separation was achieved in a Buckyprep column, using toluene:methanol
413 (90:10) as mobile phase at different temperatures (25 °C, 30 °C, 35 °C and 40 °C).

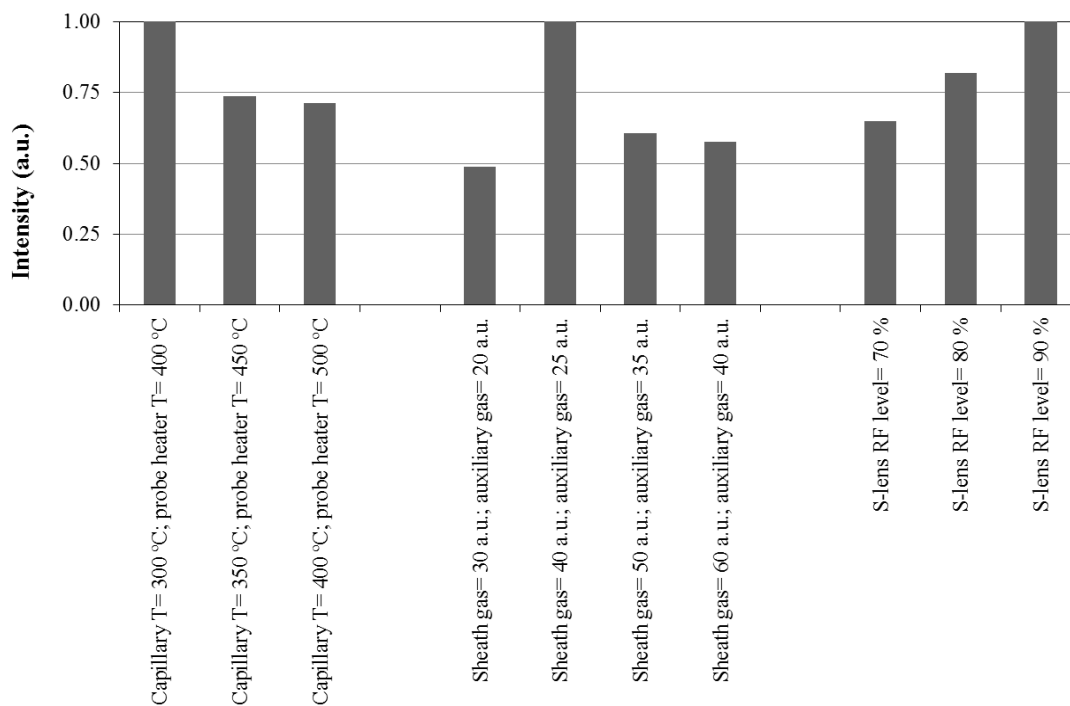


414

415

416 **Figure S4.** Normalised intensities of the $[C_{60}]^{\cdot-}$ radical ion when working at different APPI
417 conditions. Relatively low source temperatures, intermediate gas flows and high S-lens RF
418 levels resulted in the optimal performance.

419



420

Figure S5. Structures of the two molecules with formula $C_{60}O$. *a*: C_{60} epoxide ($[6,6]C_{60}O$); *b*: C_{60} oxidoannulene ($[5,6]C_{60}O$).

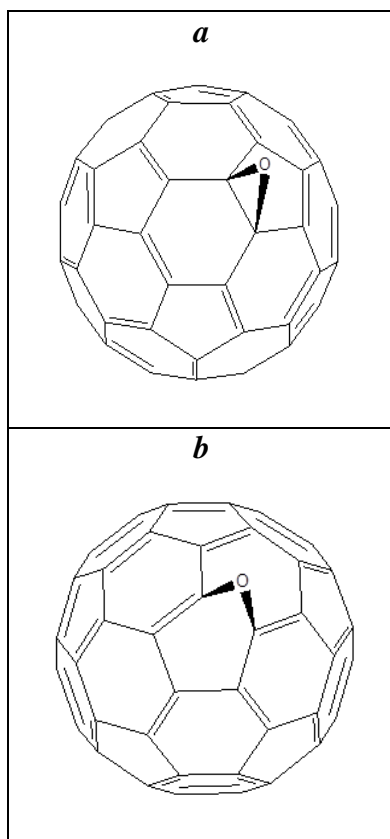


Figure S6. Structures of selected regioisomers of triepoxidized C₆₀ fullerenes (*a*, *b* and *c*).

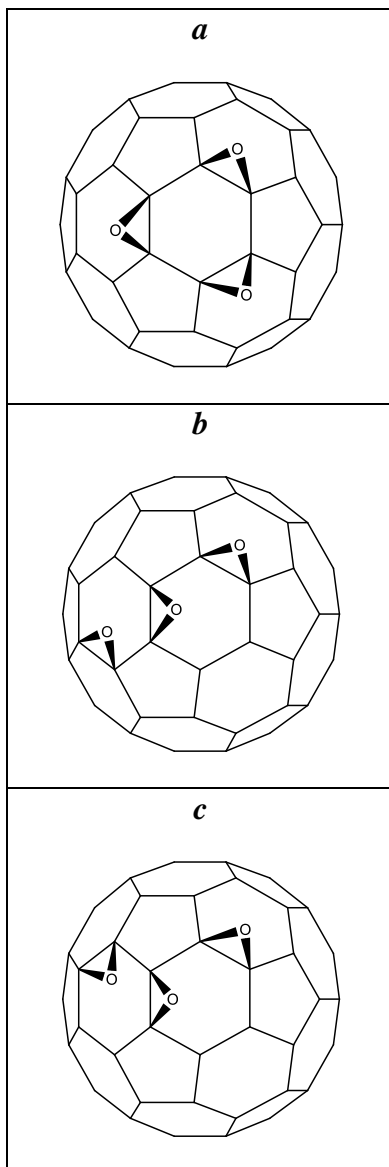


Figure S7. Structure of the most stable tetraepoxidized C_{60} fullerene.

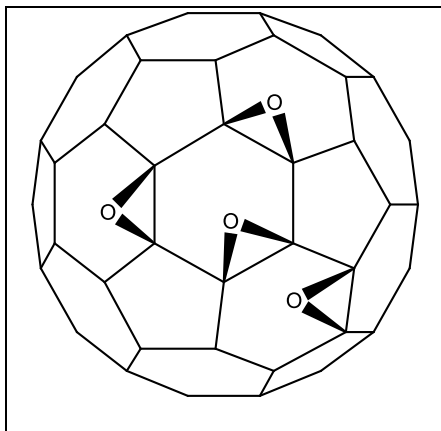


Figure S8. Signals of fullereneols observed in suspensions after sonication. Figure *a* shows a total ion chromatogram with three principal groups of signals: the peak of C₆₀ fullerene ($t_R=3.00$), a peak of overlapped fullereneols at ($t_R=1.84$) and unretained peaks near the dead volume ($t_R=1.01$). The extracted ion chromatograms of [C₆₀O]⁻, [C₆₀O₂H]⁻ and [C₆₀O₆H₅]⁻ are shown in Figure *b*, *c* and *d*.

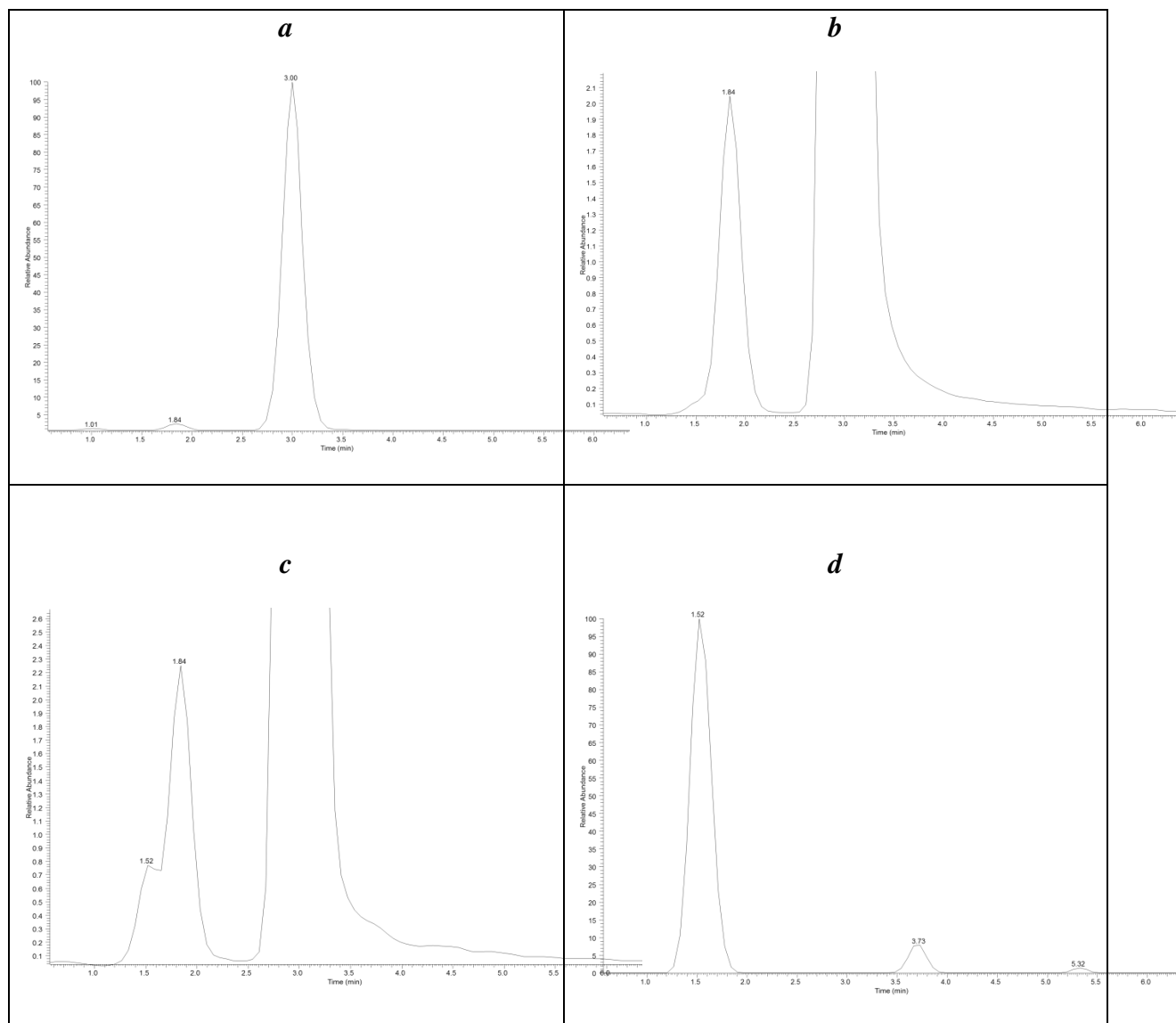


Figure S9. General scheme of reactions happening in the system.

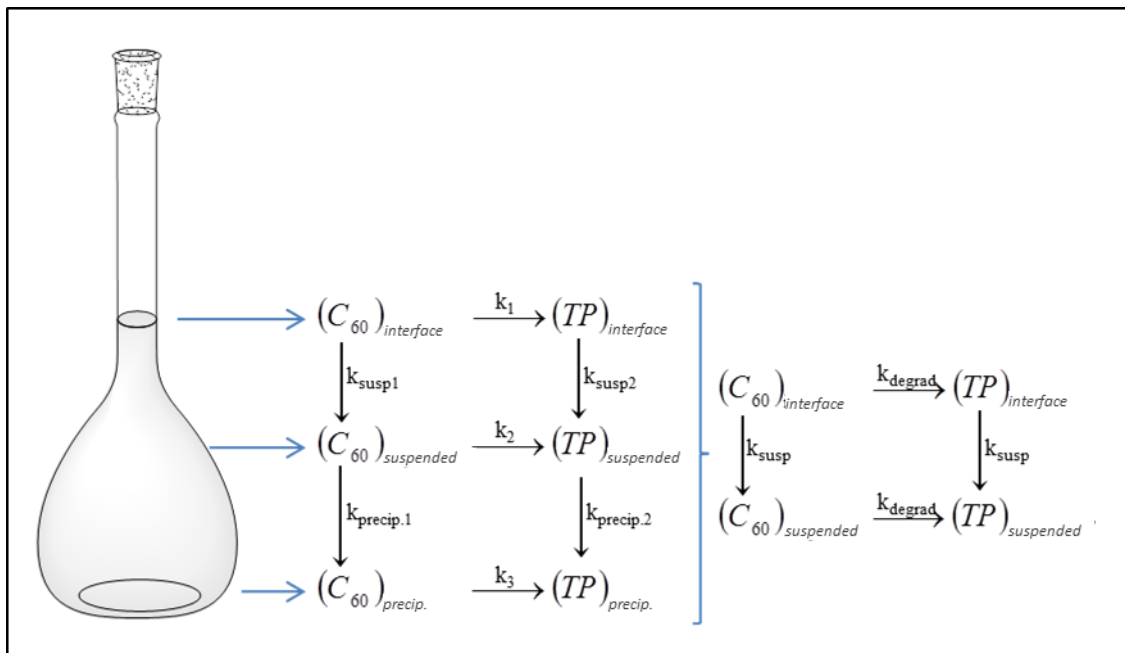


Figure S10. Generation and degradation of $C_{120}O$ and $C_{120}O_2$ in ultrapure water

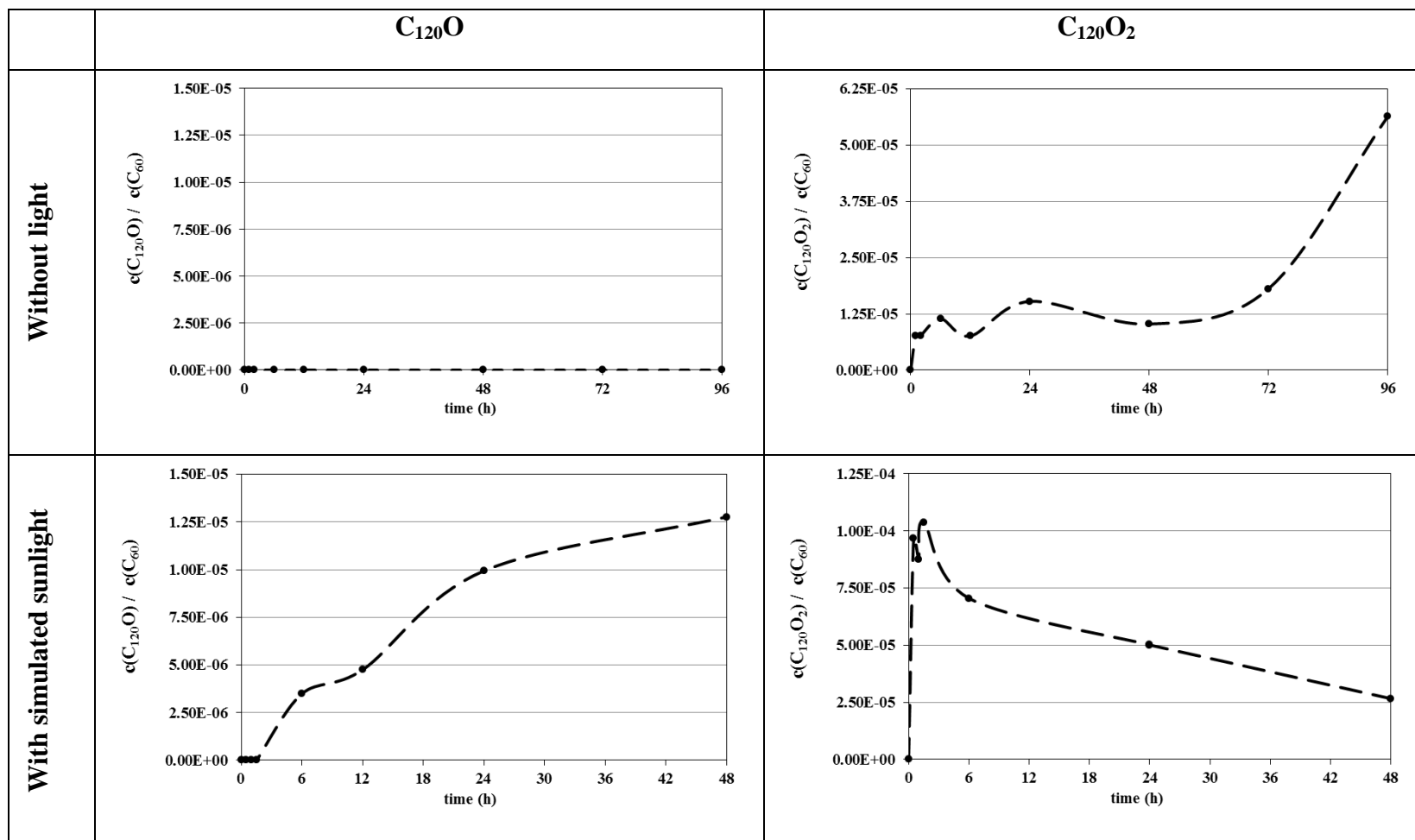


Figure S11. Impact of salinity (● = 5.8 $\mu\text{S cm}^{-1}$; ● = 970 $\mu\text{S cm}^{-1}$; ● = 46,000 $\mu\text{S cm}^{-1}$) on the generation of selected C_{60}O_x .

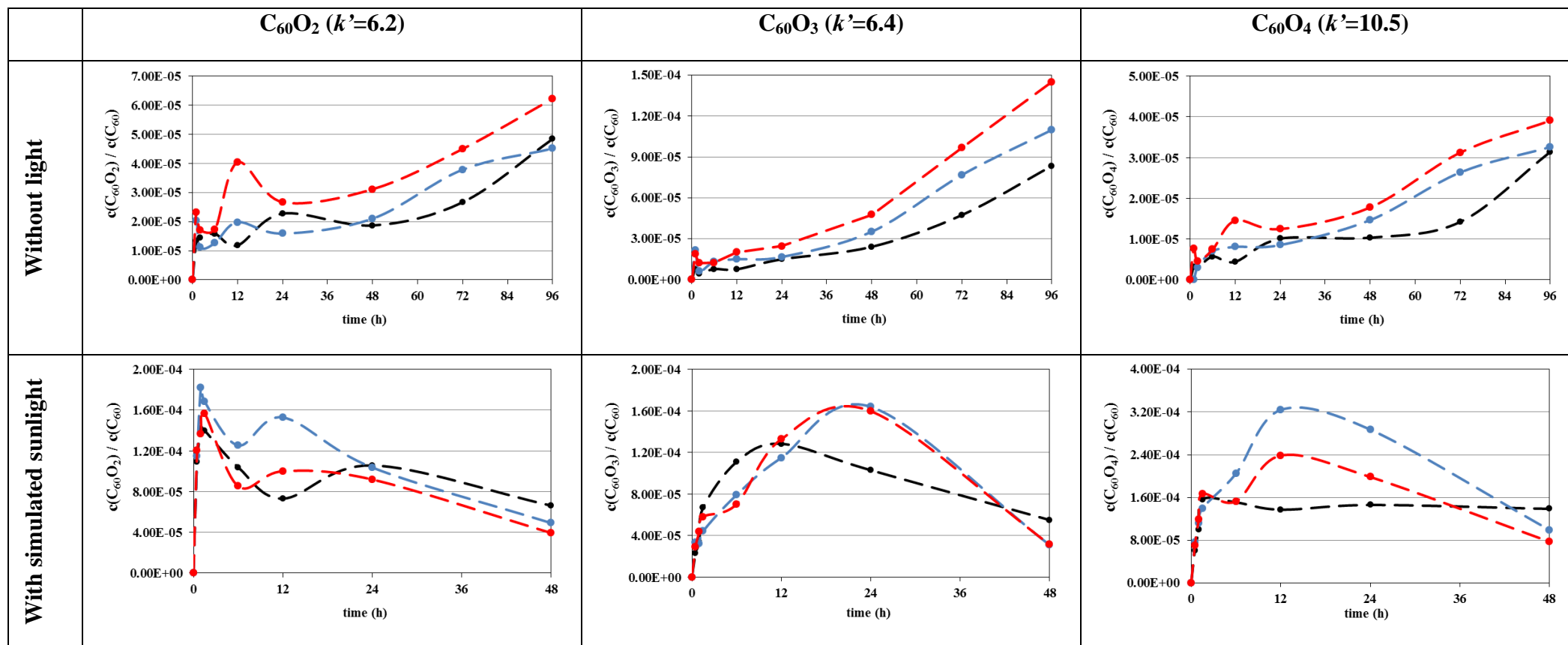


Figure S11 (cont). Impact of salinity (● = 5.8 $\mu\text{S cm}^{-1}$; ● = 970 $\mu\text{S cm}^{-1}$; ● = 46,000 $\mu\text{S cm}^{-1}$) on the generation of selected C_{120}O_x .

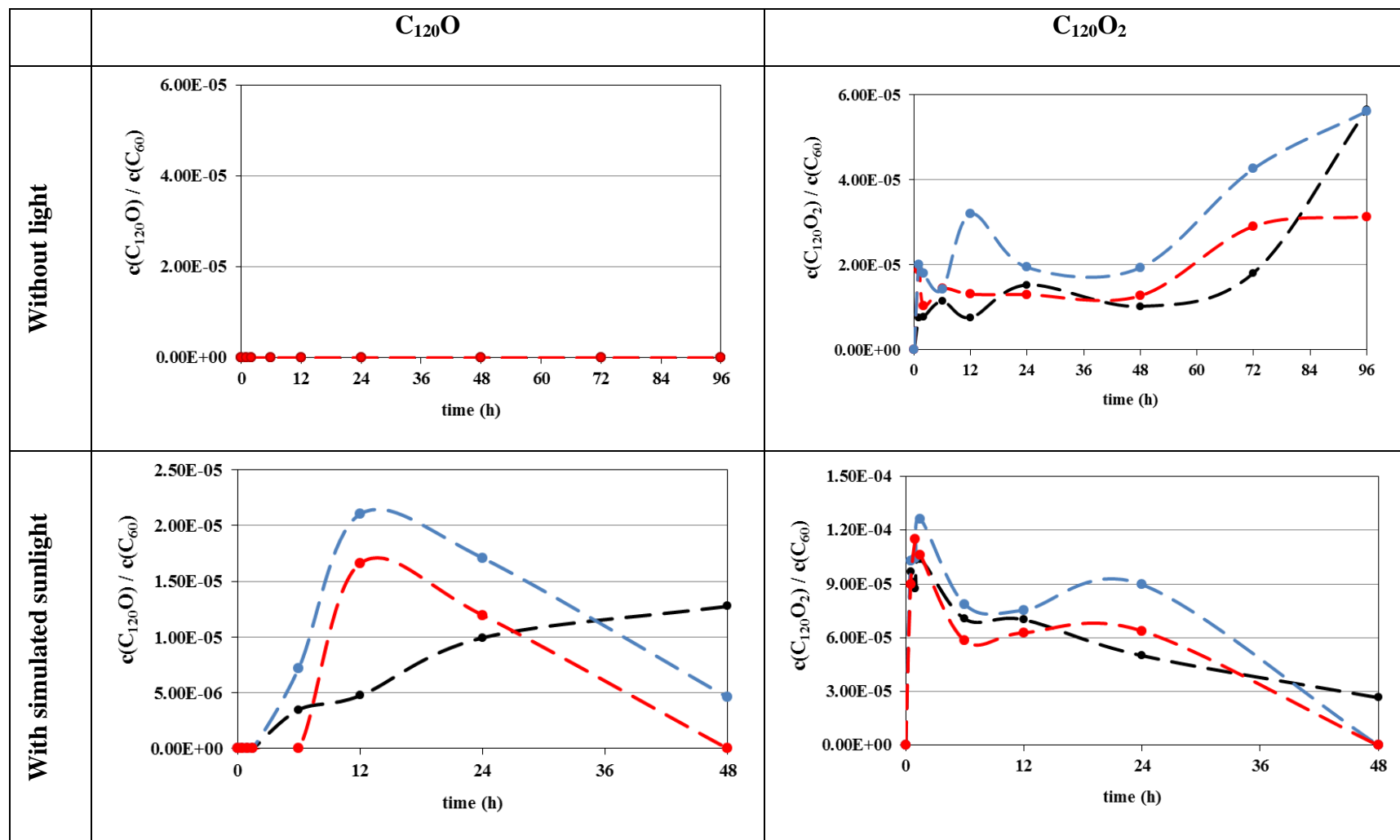


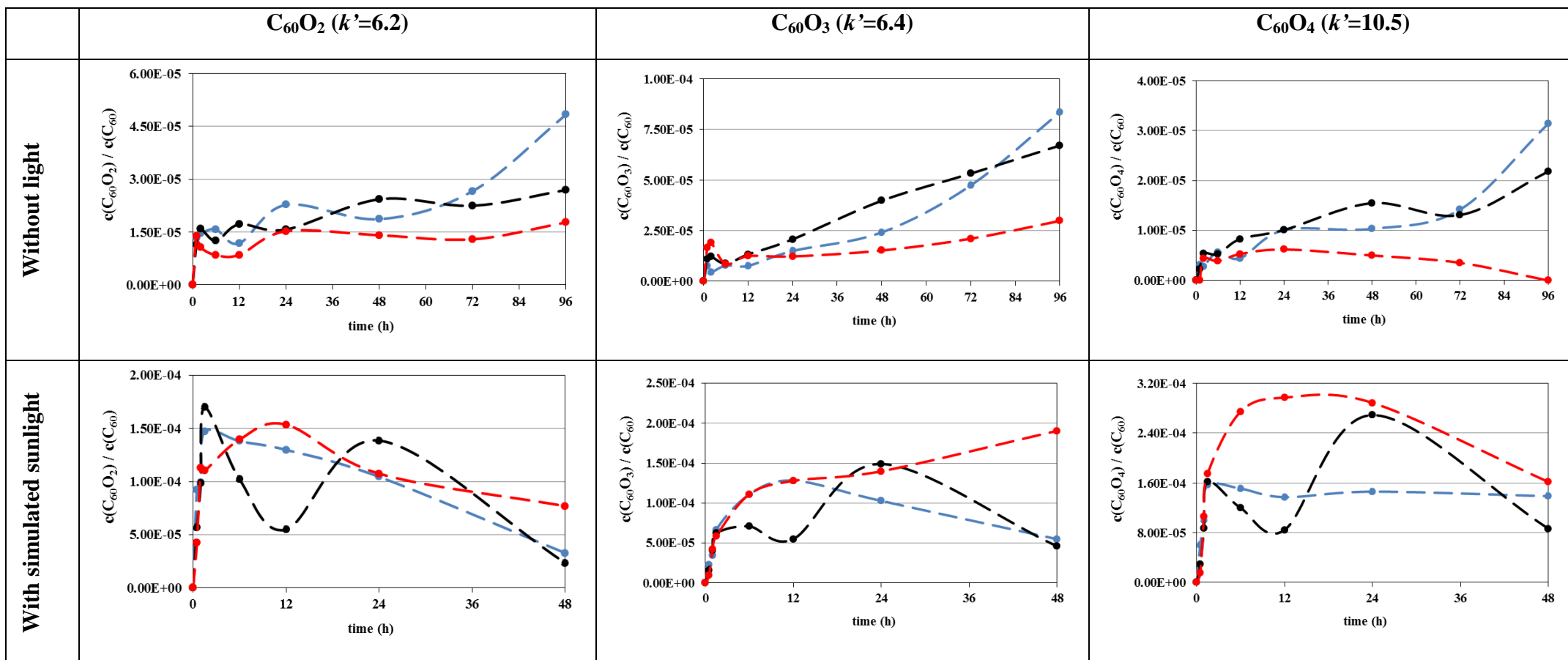
Figure S12. Impact of the pH (●: pH=6.00; ●: pH=7.00; ●: pH=8.15) on the generation of selected $C_{60}O_x$.

Figure S12(cont). Impact of the pH (●: pH=6.00; ●: pH=7.00; ●: pH=8.15) on the generation of selected $C_{120}O_x$.

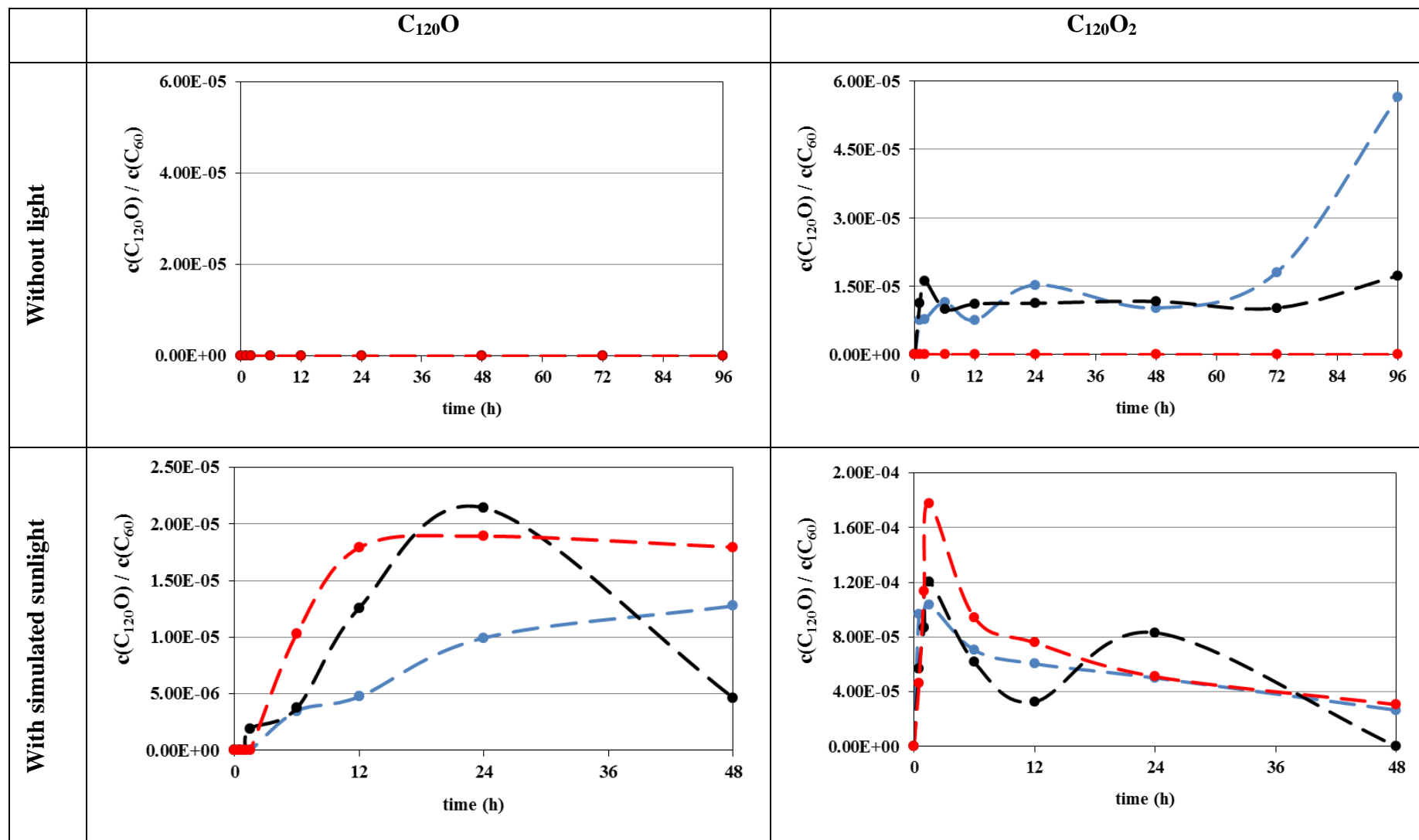


Figure S13. Impact of the humic acids content (●: [HA] = 0 mg l⁻¹; ●: [HA] = 2.25 mg l⁻¹; ●: [HA] = 0.30 mg l⁻¹) on the generation of selected C₆₀O_x.

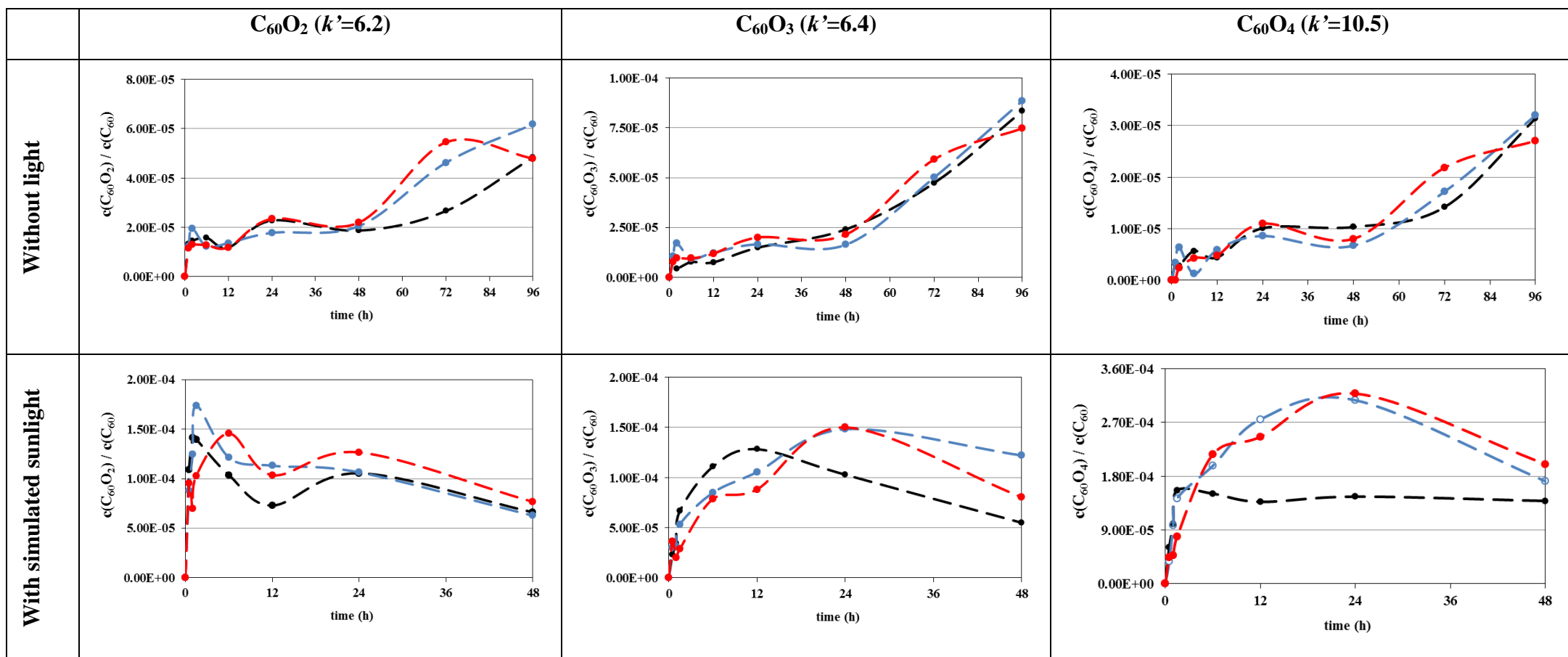


Figure S13 (cont). Impact of the humic acids content (●: [HA] = 0 mg l⁻¹; ●: [HA] = 2.25 mg l⁻¹; ●: [HA] = 0.30 mg l⁻¹) on the generation of selected C₁₂₀O_x.

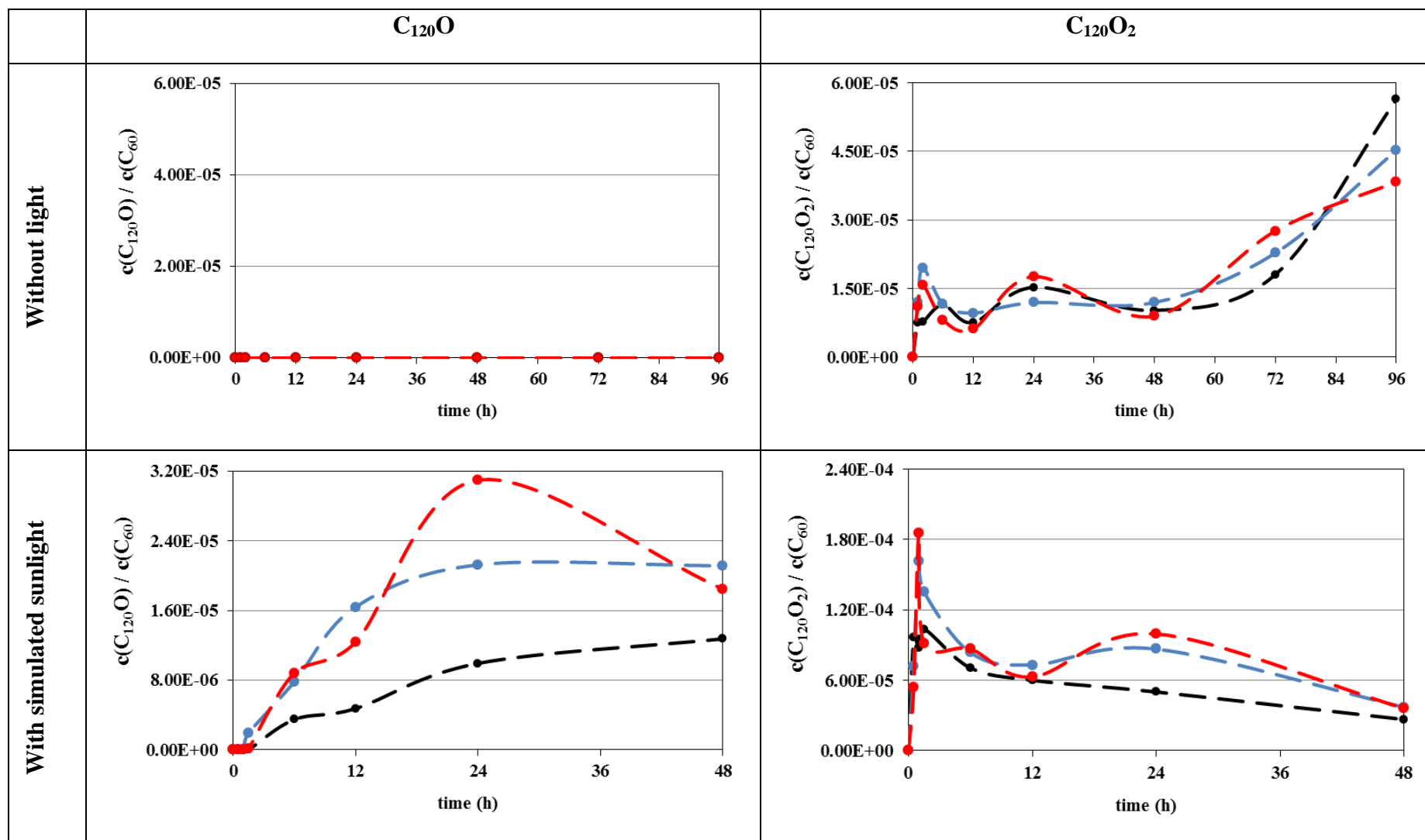
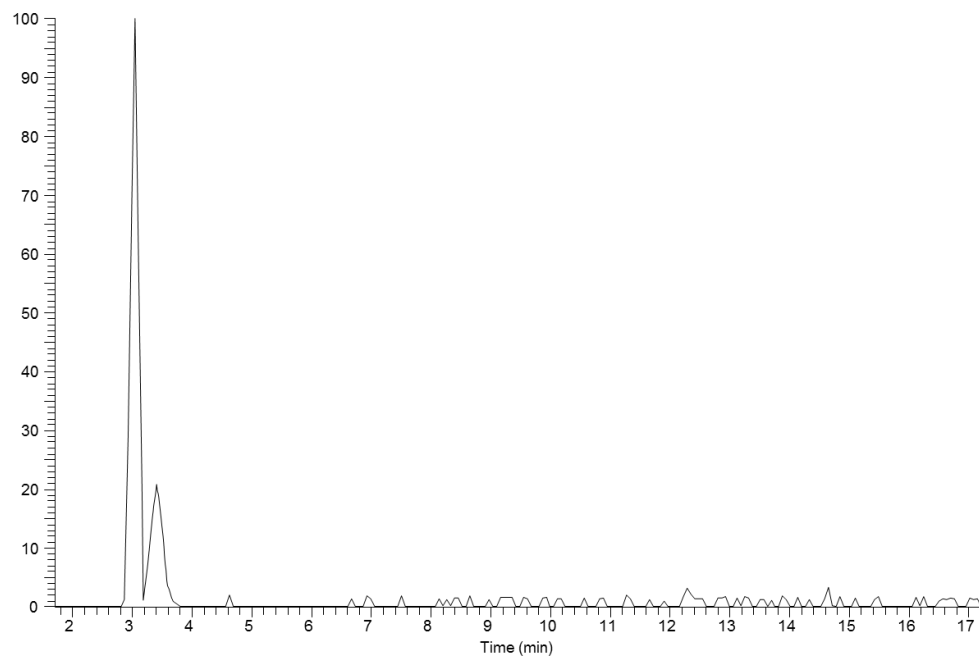


Figure S14. $C_{60}O$ signal in the extract of freshwater from the Besòs River (Barcelona). The first peak belongs to the oxidized adduct of the C_{60} molecule, while the second peak belongs to the tentatively identified transformation product.



References

- [1] D. Bouchard, X. Ma, Extraction and high-performance liquid chromatographic analysis of C60, C70, and [6,6]-phenyl C61-butyric acid methyl ester in synthetic and natural waters, *Journal of Chromatography A* 1203(2) (2008) 153-159.
- [2] A.P. van Wezel, V. Morinière, E. Emke, T. ter Laak, A.C. Hogenboom, Quantifying summed fullerene nC60 and related transformation products in water using LC LTQ Orbitrap MS and application to environmental samples, *Environment International* 37(6) (2011) 1063-1067.
- [3] Ó. Núñez, H. Gallart-Ayala, C.P.B. Martins, E. Moyano, M.T. Galceran, Atmospheric Pressure Photoionization Mass Spectrometry of Fullerenes, *Analytical Chemistry* 84(12) (2012) 5316-5326.
- [4] J. Sanchís, L.F.S. Oliveira, F.B. de Leão, M. Farré, D. Barceló, Liquid chromatography–atmospheric pressure photoionization–Orbitrap analysis of fullerene aggregates on surface soils and river sediments from Santa Catarina (Brazil), *Science of the Total Environment* 505 (2015) 172-179.
- [5] L. Li, S. Huhtala, M. Sillanpää, P. Sainio, Liquid chromatography-mass spectrometry for C60 fullerene analysis: optimisation and comparison of three ionisation techniques, *Analytical and bioanalytical chemistry* 403(7) (2012) 1931-1938.